International Applied Mechanics, Vol. 43, No. 6, 2007

To the Beginning of the Third Millennium

MESOMECHANICS OF DEFORMATION AND SHORT-TERM DAMAGE OF LINEAR ELASTIC HOMOGENEOUS AND COMPOSITE MATERIALS

L. P. Khoroshun and E. N. Shikula

UDC 539.3

The structural theory of microdamage of homogeneous and composite materials is generalized. The theory is based on the equations and methods of the mechanics of microinhomogeneous bodies with stochastic structure. A single microdamage is modeled by a quasispherical pore empty or filled with particles of a damaged material. The accumulation of microdamages under increasing loading is modeled as increasing porosity. The damage within a single microvolume is governed by the Huber–Mises or Schleicher–Nadai failure criterion. The ultimate strength is assumed to be a random function of coordinates with power-law or Weibull one-point distribution. The stress–strain state and effective elastic properties of a composite with microdamaged components are determined using the stochastic equations of elasticity. The equations of deformation and microdamage and the porosity balance equation constitute a closed-form system of equations. The solution is found iteratively using conditional moments. The effect of temperature on the coupled processes of deformation and microdamage is taken into account. Algorithms for plotting the dependences of microdamage and macrostresses on macrostrains for composites of different structure are developed. The effect of temperature and strength of damaged material on the stress–strain and microdamage curves is examined

Keywords: composite material, stochastic structure, deformation, short-term damage, porosity, temperature, effective elastic properties, stress–strain state

Introduction. One of the possible failure mechanisms in materials and structural members is associated with damage accumulation, which generally leads to the occurrence and development of main cracks. Physically, the damage of a material is dispersed defects in the form of vacancies, microcracks, microvoids, or destroyed microvolumes, which reduce the effective or load-bearing portion of the material. Thus, the damaged portion of the material can be considered a component with structural elements having zero load-bearing capacity, arranged chaotically, and characterized by some volume fraction, dimensions, orientation, and cohesion.

Damage accumulation is a rather complicated physical process dependent on the stress–strain state, temperature, chemical and radiation influences, and the structure and mechanical properties of the material. Experimental data on and observation of the behavior of structural members and structures indicate that damage may be both short-term or instantaneous (corresponding to the level of stress or strain at the moment of load application) and long-term (increasing after load application).

Damages in the form of dispersed submicrocracks, their dimensions and shape, dependence on types of loading have been well studied for polymer materials [31]. Damage formation in a number of polymers follows certain patterns. The dimensions of submicrocracks are practically independent of strain, stress, and time under load. The ratio of the longitudinal

S. P. Timoshenko Institute of Mechanics, National Academy of Sciences of Ukraine, Kyiv. Translated from Prikladnaya Mekhanika, Vol. 43, No. 6, pp. 3–42, June 2007. Original article submitted December 3, 2006.

1063-7095/07/4306-0591 ©2007 Springer Science+Business Media, Inc.

(relative to the tension direction) to the transverse dimension of a submicrocrack varies from 0.4 to 1.3 in different polymers. A certain tensile strain corresponds to a certain volume fraction of submicrocracks, which increases with the strain. Submicrocracks start forming only after a certain strain level. If a tensile stress is applied, a certain number of submicrocracks form immediately, followed by at first rapid and then more slower accumulation of submicrocracks. The rate of accumulation and volume fraction of submicrocracks increase with the stress applied. Under small stresses (less than half the breaking stress), no crack accumulation is observed for a relatively long time.

The above-mentioned experimental patterns can be explained in statistical terms. At the microscopic level, the strength of a material is inhomogeneous; i.e., the ultimate short-term strength and long-term strength are random functions of coordinates with certain distribution densities or functions. When a macrospecimen is under constant tensile stress, microvolumes in which the ultimate strength is less than the stress applied will be destroyed, i.e., microcracks or microcavities will form in their places. Microvolumes where the stress is less than yet close to the ultimate strength will be destroyed in some time dependent on the difference between the applied stress and the ultimate microstrength. When there are no more microvolumes with ultimate strengths close to the applied stress, damages cease to accumulate. As the stress increases, new microvolumes with higher microstrength are destroyed. The process becomes more intensive as microstresses are redistributed because damaged microvolumes no longer resist loads.

There are three groups of mathematical models describing the damage of materials. One group is based on certain ideas of the microstructure of the material and the mechanism of formation of microdamages in the form of damaged structural elements (microcracks or micropores) [3, 6, 12, 15, 17, 18, 25–32, 38, 46, 47, 51–77]. The governing relations include the equations of the mechanics of structurally inhomogeneous media and failure criteria for separate structural elements. Another group of models is based on a formal damage parameter introduced as some measure of discontinuity of the material and on a postulated evolutionary equation relating the rate of damage accumulation and the stresses [1, 7–9, 13, 14, 23, 24]. The physical meaning of damage and its mechanism are not always indicated. The third group is based on the assumption that damage is described by some state variables that together with stresses and strains contribute to the laws of thermodynamics. This makes it possible to formally write relations among stresses, strains, and damage parameters [2, 5, 16, 21, 22, 48, 49].

The models of the first group, which consider that the microinhomogenity of the material is the cause of dispersed microdamages, most adequately describe real damage processes. The stochastic inhomogeneity of microstrength inherent in real materials and described by probability distributions allows us to explain and model the short-term (instantaneous) damage manifested under high loads. The mathematical theory of short-term damage [51, 52] models destroyed microvolumes by randomly dispersed micropores (empty or filled with destroyed material) and uses stochastic equations of elasticity to describe the microdeformation and effective elastic properties of the porous material. The damage within a single microvolume is governed by the Huber–Mises or Schleicher–Nadai failure criterion where the ultimate strength is a random function of coordinates with a given statistically homogeneous one-point distribution having the property of ergodicity. Proceeding from the general property of the one-point distribution function of the ergodic random field of ultimate microstrength, we derived the microdamage (porosity) balance equation relating porosity and macrostresses or macrostrains. The macrostress–macrostrain relationship with porosity-dependent effective elastic constants and the porosity balance equation constitute a closed-form system of equations that describes the coupled processes of deformation and damage, which leads to a nonlinear dependence of macrostrains on macrostresses. The coupled processes of deformation and damage were investigated for both homogeneous [51, 52, 65] and composite materials [38–43, 46, 47, 51–64, 66–76] with linear and nonlinear elastic components under mechanical and thermal forces.

The theory of the coupled processes of deformation and short-term damage describes the interaction of mechanical phenomena at different structural levels: two levels for homogeneous materials (macrodeformation of the porous material and microdamage in the undamaged material) and three levels for composite materials (macrodeformation of the composite, deformation of porous portions of its components, and microdamage in the undamaged portions of the components). In view of the classification and terminology adopted in solid mechanics [50], there is good reason to associate this theory with mesomechanics, which studies mechanical phenomena at different structural levels.

The present paper systematizes studies on mathematical models that describe the coupled processes of deformation and short-term microdamage of linear elastic homogeneous and composite materials with stochastic structure. These studies were completed at the Institute of Mechanics, National Academy of Sciences of Ukraine, over the period from 1998 to 2002.

1. Short-Term Damage of Materials with Microdamages Modeled by Empty Pores.

1.1. Homogeneous Material. Consider an elementary structural model where dispersed microdamages are represented by randomly arranged quasispherical empty micropores. Macrostresses and macrostrains in a homogeneous material with microdamage described by porosity p are related by

$$\langle\sigma_{ij}\rangle = (K^* - 2/3\mu^*)\langle\varepsilon_{rr}\rangle\delta_{ij} + 2\mu^*\langle\varepsilon_{ij}\rangle, \tag{1.1}$$

where the effective bulk, K^*, and shear, μ^*, moduli are defined, according to the theory of porous media [33, 35], by the formulas

$$K^* = \frac{4K\mu(1-p)^2}{4\mu + (3K - 4\mu)p}, \quad \mu^* = \frac{(9K + 8\mu)\mu(1-p)^2}{9K + 8\mu - (3K - 4\mu)p}, \tag{1.2}$$

where K and μ are the bulk and shear moduli of the undamaged portion (skeleton) of the material.

The following formulas will be useful in further derivations:

$$K^* = \frac{4(1+\nu)\mu(1-p)^2}{3[2(1-2\nu)-(1-5\nu)p]}, \quad \mu^* = \frac{(7-5\nu)\mu(1-p)^2}{7-5\nu+(1-5\nu)p},$$

$$\nu^* = \frac{2\nu(7-5\nu)+(1-5\nu)(3-\nu)p}{2(7-5\nu)-(1-5\nu)(1-3\nu)p}, \tag{1.3}$$

where ν^* is the effective Poisson's ratio and ν is Poisson's ratio for the undamaged portion of the material.

A single microdamage occurs in the undamaged material in accordance with the Huber–Von Mises failure criterion [13]

$$I_{\bar\sigma} = k, \tag{1.4}$$

where $I_{\bar\sigma} = (\bar\sigma'_{ij}\bar\sigma'_{ij})^{1/2}$ is the second invariant of mean deviatoric stress tensor $\bar\sigma'_{ij}$ in the undamaged material, and k is the limiting value of the left-hand side of (1.4), which is a random function of coordinates.

The mean stresses $\langle\bar\sigma_{ij}\rangle'$ are related to the macrostresses by

$$\bar\sigma_{ij} = \frac{1}{1-p}\langle\sigma_{ij}\rangle. \tag{1.5}$$

Therefore, according to (1.1), we have

$$I_{\bar\sigma} = \frac{1}{1-p}I_\sigma = \frac{2\mu^*}{1-p}I_\varepsilon, \tag{1.6}$$

where

$$I_\sigma = (\langle\sigma_{ij}\rangle'\langle\sigma_{ij}\rangle')^{1/2}, \quad I_\varepsilon = (\langle\varepsilon_{ij}\rangle'\langle\varepsilon_{ij}\rangle')^{1/2}. \tag{1.7}$$

The one-point distribution function $F(k)$ of the ultimate strength k in a microvolume of the undamaged material may be approximated by a power-law function on some interval

$$F(k) = \begin{cases} 0, & k < k_0, \\ \left(\dfrac{k-k_0}{k_1-k_0}\right)^n, & k_0 \le k \le k_1, \\ 1, & k > k_1, \end{cases} \tag{1.8}$$

or by the Weibull function

$$F(k)=\begin{cases}0, & k<k_0,\\ 1-\exp\left[-m(k-k_0)^n\right], & k\ge k_0,\end{cases} \tag{1.9}$$

where k_0 is the minimum value of k; k_1, m, and n are constants that provide the best fit to experimental strength scatter or stress–strain curves.

Let the material have some initial porosity p_0 prior to loading. We assume that the random field of ultimate strength k is statistically homogeneous, which is characteristic of real materials, and the size of single microdamages and distances among them are negligible compared with the macrovolume of the material. Then, since the random field of k is ergodic [35], the function $F(k)$ defines the volume fraction of the skeleton in which the ultimate strength is less than k. Therefore, when $\overline{\sigma}'_{ij}$, the function $F(I_{\overline{\sigma}})$ defines the volume fraction of the destroyed microvolumes of the skeleton, according to (1.4), (1.8), and (1.9). Since destroyed microvolumes are modeled by pores, we have the following porosity balance equation [51]:

$$p=p_0+(1-p_0)F(I_{\overline{\sigma}}). \tag{1.10}$$

In view of (1.6), (1.7), Eq. (1.10) reduces to the following form when macrostresses $\langle\sigma_{ij}\rangle$ or macrostrains $\langle\varepsilon_{ij}\rangle$ are given:

$$p=p_0+(1-p_0)F\left(\frac{1}{1-p}I_\sigma\right),\qquad p=p_0+(1-p_0)F\left(\frac{2\mu^*}{1-p}I_\varepsilon\right). \tag{1.11}$$

Relations (1.1), (1.2), and (1.11) constitute a closed-form system of equations that describes the coupled processes of statistically homogeneous deformation and damage of a material with microdamages modeled by empty pores. Specifying the macrostrains $\langle\varepsilon_{ij}\rangle$, we can find the porosity p from the nonlinear equations (1.2) and (1.11). Then, substituting p into (1.1) and (1.2), we obtain a nonlinear relation between $\langle\sigma_{ij}\rangle$ and $\langle\varepsilon_{ij}\rangle$. Since Eqs. (1.2) and (1.11) are nonlinear, their general solution can be found by iterative methods.

1.2. Particulate Composite. Consider a particulate composite whose inclusions and matrix have porosities p_1 and p_2, respectively. Denote the bulk and shear moduli of the skeletons of the inclusions and matrix by K_1,μ_2 and K_2,μ_2 and the volume fractions of the porous inclusions and porous matrix by c_1 and c_2, respectively. If the macrostrains $\langle\varepsilon_{pq}\rangle$ are given, then the macrostresses $\langle\sigma_{pq}\rangle$ are expressed as

$$\langle\sigma_{ij}\rangle=(K^*-2/3\mu^*)\langle\varepsilon_{rr}\rangle\delta_{ij}+2\mu^*\langle\varepsilon_{ij}\rangle, \tag{1.12}$$

where the effective bulk, K^*, and shear, μ^*, moduli of the composite are defined [10, 34, 35, 37] in terms of the analogous moduli of the porous inclusions (K_1^*,μ_1^*) and porous matrix (K_2^*,μ_2^*):

$$K^*=c_1K_1^*+c_2K_2^*-\frac{c_1c_2(K_1^*-K_2^*)^2}{c_1K_2^*+c_2K_1^*+n_c},\qquad \mu^*=c_1\mu_1^*+c_2\mu_2^*-\frac{c_1c_2(\mu_1^*-\mu_2^*)^2}{c_1\mu_2^*+c_2\mu_1^*+m_c}, \tag{1.13}$$

where

$$n_c=\frac{4}{3}\mu_c,\qquad m_c=\frac{(9K_c+8\mu_c)\mu_c}{6(K_c+2\mu_c)}, \tag{1.14}$$

$$K_c=c_1K_1^*+c_2K_2^*,\qquad \mu_c=c_1\mu_1^*+c_2\mu_2^*, \tag{1.15}$$

if the matrix is stiffer than the inclusions, and

$$K_c=\frac{K_1^*K_2^*}{c_1K_2^*+c_2K_1^*},\qquad \mu_c=\frac{\mu_1^*\mu_2^*}{c_1\mu_2^*+c_2\mu_1^*} \tag{1.16}$$

otherwise.

According to [33], K_1^*, μ_1^* and K_2^*, μ_2^* are defined by

$$K_{ip} = \frac{4K_i \mu_i (1-p_i)^2}{4\mu_i + (3K_i - 4\mu_i) p_i}, \quad \mu_{ip} = \frac{(9K_i + 8\mu_i)\mu_i (1-p_i)^2}{9K_i + 8\mu_i - (3K_i - 4\mu_i) p_i} \quad (i = 1, 2). \tag{1.17}$$

A single microdamage occurs in the undamaged portion of the *i*th component in accordance with the Huber–Von Mises failure criterion [13]:

$$I_{\bar{\sigma}}^i = k_i, \quad I_{\bar{\sigma}}^i = (\bar{\sigma}_{pq}'^i \, \bar{\sigma}_{pq}'^i)^{1/2} \quad (i = 1, 2), \tag{1.18}$$

where $\bar{\sigma}_{pq}'^i$ are the mean deviatoric stresses in the undamaged portion of the *i*th component; k_i is the limiting value of the left-hand side of (1.18) for the *i*th component, which is a random function of coordinates.

The one-point distribution function of k_i may be approximated by a power-law function on a finite interval

$$F_i(k_i) = \begin{cases} 0, & k_i < k_{0i}, \\ \left(\dfrac{k_i - k_{0i}}{k_{1i} - k_{0i}} \right)^{\alpha_i}, & k_{0i} \le k_i \le k_{1i}, \\ 1, & k_i > k_{1i}, \end{cases} \tag{1.19}$$

or by the Weibull function

$$F_i(k_i) = \begin{cases} 0, & k_i < k_{0i}, \\ 1 - \exp\left[-m_i (k_i - k_{0i})^{\alpha_i} \right], & k_i \ge k_{0i}, \end{cases} \tag{1.20}$$

where k_{0i} is the minimum value of k_i at which damage begins in some volumes of the *i*th component; k_{1i}, m_i, and α_i are constants chosen from the strength scatter condition for the *i*th component.

Let the *i*th component of the composite have initial microdamage characterized by a porosity p_{0i}. Then the distribution function $F_i(k_i)$ defines the volume fraction of the undamaged material in the *i*th component in which the ultimate strength is less than k_i. Therefore, if the stresses in the undamaged portion of the *i*th component are equal to $\bar{\sigma}_{pq}^i$, then the function $F_i(\bar{I}_{\sigma}^i)$ defines the volume fraction of destroyed microvolumes of the skeleton of the *i*th component, according to (1.18)–(1.20). Since destroyed microvolumes are modeled by pores, we have the following porosity balance equation [51, 53]:

$$p_i = p_{0i} + (1 - p_{0i}) F_i(I_{\bar{\sigma}}^i), \tag{1.21}$$

where

$$I_{\bar{\sigma}}^i = \frac{2\mu_i^*}{1-p_i} I_{\langle\varepsilon\rangle}^i, \quad I_{\langle\varepsilon\rangle}^i = (\langle \varepsilon_{ij}^i \rangle' \langle \varepsilon_{ij}^i \rangle')^{1/2} \tag{1.22}$$

and, moreover,

$$I_{\langle\varepsilon\rangle}^i = (-1)^{i+1} \frac{\mu^* - \mu_{3-i}^*}{c_i (\mu_1^* - \mu_2^*)} I_{\langle\varepsilon\rangle}. \tag{1.23}$$

In view of (1.22), (1.23), Eq. (1.21) reduces to the following form when $\langle \varepsilon_{ij} \rangle$ are given:

$$p_i = p_{0i} + (1 - p_{0i}) F_i \left(\frac{2\mu_{ip}}{1-p_i} I_{\langle\varepsilon\rangle}^i \right) = p_{0i} + (1 - p_{0i}) F_i \left((-1)^{i+1} \frac{2\mu_{ip} (\mu^* - \mu_{(3-i)p})}{(1-p_i) c_i (\mu_{1p} - \mu_{2p})} I_{\langle\varepsilon\rangle} \right), \tag{1.24}$$

where K_{1p}, μ_{1p} and K_{2p}, μ_{2p} are defined by (1.17).

Relations (1.13)–(1.19), (1.21)–(1.23) or (1.13)–(1.18), (1.20)–(1.23) can be used as the basis for an iterative algorithm of determining the volume fraction of microdamages in the components and the elastic characteristics of the composite. To this end, we will use the secant method [4].

After rearranging the porosity balance equation (1.21) into the form

$$\varphi_i(p_i) = \left[p_i - p_{0i} + (1 - p_{0i}) F_i \left(\frac{2\mu_{ip}}{1 - p_i} I^i_{\langle \varepsilon \rangle} \right) \right] = 0, \tag{1.25}$$

it can be verified that the root p_i falls into the interval $[p_{0i}, 1]$ because

$$\varphi_i(p_{0i}) < 0, \quad \varphi_i(1) > 0. \tag{1.26}$$

Therefore, the zero-order approximation of the root $p_i^{(0)}$ is determined by the formula

$$p_i^{(0)} = \frac{a_i^{(0)} \varphi_i(b_i^{(0)}) - b_i^{(0)} \varphi_i(a_i^{(0)})}{\varphi_i(b_i^{(0)}) - \varphi_i(a_i^{(0)})}, \tag{1.27}$$

where $a_i^{(0)} = p_{0i}$ and $b_i^{(0)} = 1$. The subsequent approximations are determined in the iterative process

$$p_i^{(m)} = \frac{a_i^{(m)} \varphi_i(b_i^{(m)}) - b_i^{(m)} \varphi_i(a_i^{(m)})}{\varphi_i(b_i^{(m)}) - \varphi_i(a_i^{(m)})}, \tag{1.28}$$

$$a_i^{(m)} = a_i^{(m-1)}, \quad b_i^{(m)} = p_i^{(m-1)} \quad \text{for} \quad \varphi_i(a_i^{(m-1)}) \varphi_i(p_i^{(m-1)}) \le 0,$$

$$a_i^{(m)} = p_i^{(m-1)}, \quad b_i^{(m)} = b_i^{(m-1)} \quad \text{for} \quad \varphi_i(a_i^{(m-1)}) \varphi_i(p_i^{(m-1)}) \ge 0 \quad (m = 1, 2, \ldots),$$

which proceeds until

$$\left| \varphi_i(p_i^{(m)}) \right| < \varepsilon, \tag{1.29}$$

where ε is the error of computing the root.

We have plotted stress–strain curves for particulate composites with microdamaged matrix for the Weibull distribution (1.20) and the following macroparameters:

$$\langle \varepsilon_{11} \rangle \ne 0, \quad \langle \sigma_{22} \rangle = \langle \sigma_{33} \rangle = 0. \tag{1.30}$$

In this case, according to (1.12), the macrostresses $\langle \sigma_{11} \rangle$ and the macrostrains $\langle \varepsilon_{11} \rangle$ are related by

$$\langle \sigma_{11} \rangle = \frac{3K^* \mu^* \langle \varepsilon_{11} \rangle}{K^* + 1/3\mu^*} \tag{1.31}$$

and

$$I_{\langle \varepsilon \rangle} = \sqrt{\frac{3}{2}} \frac{K^* \langle \varepsilon_{11} \rangle}{K^* + 1/3\mu^*} \tag{1.32}$$

in the porosity balance equation (1.24), which is equivalent to condition (1.30).

The inclusions are made of aluminoborosilicate glass with the following elastic characteristics [10] and volume fractions:

$$E_1 = 70 \text{ GPa}, \quad \nu_1 = 0.2, \quad c_1 = 0, 0.25, 0.5, 0.75, 1.00. \tag{1.33}$$

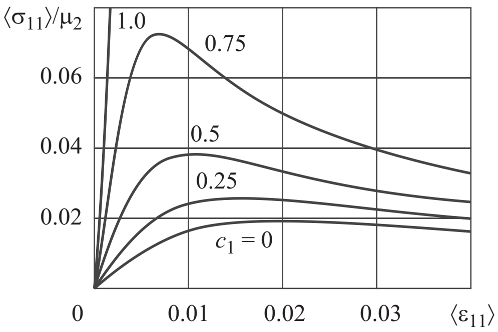

Fig. 1

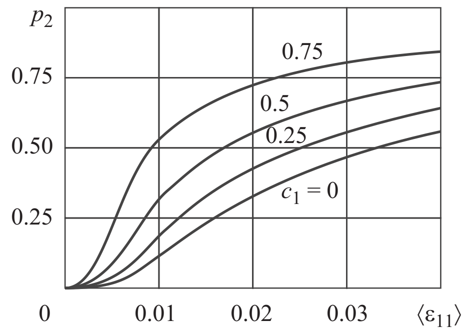

Fig. 2

The matrix is made of epoxy resin with the following elastic characteristics of the undamaged portion [20]:

$$E_2 = 3 \text{ GPa}, \quad \nu_2 = 0.35, \tag{1.34}$$

where E_1 and E_2 are Young's moduli and ν_1 and ν_2 are Poisson's ratios of the undamaged portion of the inclusions and matrix, respectively. Moreover,

$$p_{02} = 0, \quad k_{02} / \mu_2 = 0.01, \quad m_2 = 1000, \quad n_2 = 2, \quad \alpha_2 = 0.2, \quad \sigma_{2p} = 0.007 \text{ GPa}. \tag{1.35}$$

Figure 1 shows plots of the macrostress $\langle\sigma_{11}\rangle / \mu_2$ as a function of the macrostrain $\langle\varepsilon_{11}\rangle$. The curves include a linear ascending section and a nonlinear descending section (caused by microdamage) for all values of the volume fraction $c_1 < 1$. Figure 2 shows plots of the porosity p_2 as a function of the macrostrain $\langle\varepsilon_{11}\rangle$. Both figures demonstrate significant dependence on c_1.

1.3. Laminated Composite. Consider a laminated material with N isotropic components and dispersed microdamages characterized by porosity p_i $(i = 1, \ldots, N)$. Denote the bulk and shear moduli of the undamaged portion of the ith component by K_i and μ_i and the volume fractions of the porous ith component by c_i. If the macrostrains $\langle\varepsilon_{jk}\rangle$ are given, then the macrostresses $\langle\sigma_{jk}\rangle$ are expressed as

$$\langle\sigma_{jk}\rangle = (\lambda_{11}^* - \lambda_{12}^*)\langle\varepsilon_{jk}\rangle + (\lambda_{12}^*\langle\varepsilon_{rr}\rangle + \lambda_{13}^*\langle\varepsilon_{33}\rangle)\delta_{jk},$$

$$\langle\sigma_{33}\rangle = \lambda_{13}^*\langle\varepsilon_{rr}\rangle + \lambda_{33}^*\langle\varepsilon_{33}\rangle, \quad \langle\sigma_{j3}\rangle = 2\lambda_{44}^*\langle\varepsilon_{j3}\rangle \quad (j,k,r = 1,2), \tag{1.36}$$

where the effective moduli of elasticity $\lambda_{11}^*, \lambda_{12}^*, \lambda_{13}^*, \lambda_{33}^*$, and λ_{44}^* are defined by the following formulas [10, 34, 35, 37]:

$$\lambda_{11}^* = \left\langle \frac{1}{\lambda^* + 2\mu^*} \right\rangle^{-1} \left\langle \frac{\lambda^*}{\lambda^* + 2\mu^*} \right\rangle^2 + 4\left\langle \frac{\mu^*(\lambda^* + \mu^*)}{\lambda^* + 2\mu^*} \right\rangle,$$

$$\lambda_{12}^* = \left\langle \frac{1}{\lambda^* + 2\mu^*} \right\rangle^{-1} \left\langle \frac{\lambda^*}{\lambda^* + 2\mu^*} \right\rangle^2 + 2\left\langle \frac{\lambda^*\mu^*}{\lambda^* + 2\mu^*} \right\rangle,$$

$$\lambda_{13}^* = \left\langle \frac{1}{\lambda^* + 2\mu^*} \right\rangle^{-1} \left\langle \frac{\lambda^*}{\lambda^* + 2\mu^*} \right\rangle, \quad \lambda_{33}^* = \left\langle \frac{1}{\lambda^* + 2\mu^*} \right\rangle^{-1}, \quad \lambda_{44}^* = \left\langle \frac{1}{\mu^*} \right\rangle^{-1}, \tag{1.37}$$

where

$$\lambda_i^* = K_i^* - 2/3\mu_i^*, \quad \langle f^*\rangle = \sum_{i=1}^{N} c_i f_i^* \quad (i = 1, \ldots, N). \tag{1.38}$$

The effective moduli K_{ip} and μ_{ip} of the porous ith component are defined by (1.17) ($i=1,\dots,N$), according to [33].

A single microdamage occurs in the undamaged portion of the ith component in accordance with the Huber–Von Mises failure criterion (1.18) ($i=1,\dots,N$). The one-point distribution function of k_i may have the form of (1.19) or (1.20).

From the same considerations as in Sec. 1.2, we can write the equation of balance of destroyed microvolumes in (or porosity of) the ith component [51, 54] in the form (1.21) where $\overline{\sigma}^i_{jk}$ and $\langle \sigma^i_{jk}\rangle$ are related by

$$I^i_{\overline{\sigma}} = \frac{1}{1-p_i} I^i_{\langle\sigma\rangle}, \qquad I^i_{\langle\sigma\rangle} = (\langle\sigma^i_{jk}\rangle'\langle\sigma^i_{jk}\rangle')^{1/2}. \tag{1.39}$$

In view of (1.39), the porosity balance equation (1.21) becomes

$$p_i = p_{0i} + (1-p_{0i})F_i\left(\frac{I^i_{\langle\sigma\rangle}}{1-p_i}\right), \tag{1.40}$$

where $\langle\sigma^i_{jk}\rangle$ and $\langle\varepsilon_{jk}\rangle$ are related by the following formulas [10, 34, 35, 37]:

$$\langle\sigma^i_{jk}\rangle = 2\mu_{ip}\langle\varepsilon_{jk}\rangle + \frac{\lambda_{ip}}{\lambda_{ip}+2\mu_{ip}}\left\langle\frac{1}{\lambda_p+2\mu_p}\right\rangle^{-1}\left(\left\langle\frac{\lambda_p}{\lambda_p+2\mu_p}\right\rangle + 2\mu_{ip}\left\langle\frac{1}{\lambda_p+2\mu_p}\right\rangle\right)\langle\varepsilon_{rr}\rangle\delta_{jk}$$

$$+\frac{\lambda_{ip}}{\lambda_{ip}+2\mu_{ip}}\left\langle\frac{1}{\lambda_p+2\mu_p}\right\rangle\langle\varepsilon_{33}\rangle\delta_{jk},$$

$$\langle\sigma^i_{33}\rangle = \left\langle\frac{1}{\lambda_p+2\mu_p}\right\rangle^{-1}\left(\left\langle\frac{\lambda_p}{\lambda_p+2\mu_p}\right\rangle\langle\varepsilon_{rr}\rangle + \langle\varepsilon_{33}\rangle\right),$$

$$\langle\sigma^i_{j3}\rangle = 2\left\langle\frac{1}{\mu_p}\right\rangle^{-1}\langle\varepsilon_{j3}\rangle \qquad (j,k,r=1,2;\ i=1,\dots,N), \tag{1.41}$$

and the effective moduli K_{ip}, λ_{ip}, and μ_{ip} are defined by (1.17).

The iterative algorithm (1.25)–(1.29) based on the secant method [4] and on (1.17), (1.37), (1.38), (1.18), (1.19) (or (1.20)), (1.39)–(1.41) was used to determine the volume fraction of microdamages in the components and the elastic characteristics of the composite and to plot stress–strain curves for a two-component laminated composite with microdamaged reinforcement under loading of different types for the Weibull distribution (1.20). The materials of the composite are the same as in the previous subsection (see (1.33)–(1.35)).

If

$$\langle\varepsilon_{11}\rangle \neq 0, \qquad \langle\sigma_{22}\rangle = \langle\sigma_{33}\rangle = 0, \tag{1.42}$$

then, according to (1.36), the macrostress $\langle\sigma_{11}\rangle$ and the macrostrain $\langle\varepsilon_{11}\rangle$ are related by

$$\langle\sigma_{11}\rangle = \frac{\lambda^*_{11}-\lambda^*_{12}}{\lambda^*_{11}\lambda^*_{33}-(\lambda^*_{13})^2}\left[(\lambda^*_{11}+\lambda^*_{12})\lambda^*_{33}-2(\lambda^*_{13})^2\right]\langle\varepsilon_{11}\rangle \tag{1.43}$$

and

$$\langle\varepsilon_{22}\rangle = \frac{(\lambda^*_{13})^2-\lambda^*_{12}\lambda^*_{33}}{\lambda^*_{11}\lambda^*_{33}-(\lambda^*_{13})^2}\langle\varepsilon_{11}\rangle, \qquad \langle\varepsilon_{33}\rangle = \frac{(\lambda^*_{12}-\lambda^*_{11})\lambda^*_{13}}{\lambda^*_{11}\lambda^*_{33}-(\lambda^*_{13})^2}\langle\varepsilon_{11}\rangle \tag{1.44}$$

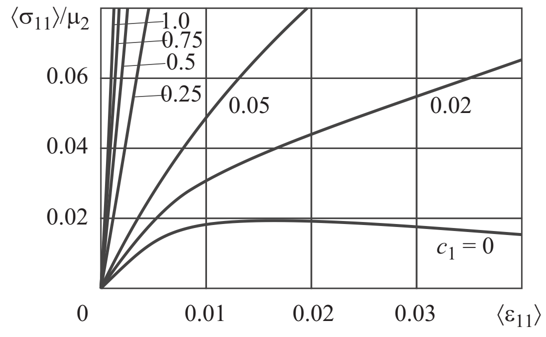

Fig. 3

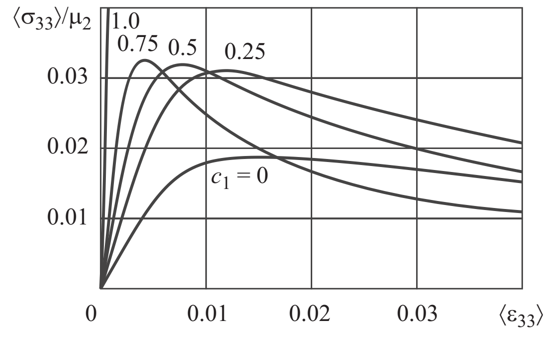

Fig. 4

in the porosity balance equation (1.40).

If

$$\langle \varepsilon_{33} \rangle \neq 0, \quad \langle \sigma_{11} \rangle = \langle \sigma_{22} \rangle = 0, \tag{1.45}$$

then, according to (1.36), the macrostress $\langle \sigma_{33} \rangle$ and the macrostrain $\langle \varepsilon_{33} \rangle$ are related by

$$\langle \sigma_{33} \rangle = \frac{1}{\lambda_{11}^* + \lambda_{12}^*} \left[(\lambda_{11}^* + \lambda_{12}^*)\lambda_{33}^* - 2(\lambda_{13}^*)^2 \right] \langle \varepsilon_{33} \rangle \tag{1.46}$$

and

$$\langle \varepsilon_{11} \rangle = \langle \varepsilon_{22} \rangle = -\frac{\lambda_{13}^*}{\lambda_{11}^* + \lambda_{12}^*} \langle \varepsilon_{33} \rangle \tag{1.47}$$

in the porosity balance equation (1.40).

Figures 3 and 4 show (for (1.42) and (1.45), respectively) the macrostress $\langle \sigma_{11} \rangle / \mu_2$ as a function of the macrostrain $\langle \varepsilon_{11} \rangle$ and the macrostresses $\langle \sigma_{33} \rangle / \mu_2$ as a function of the macrostrain $\langle \varepsilon_{33} \rangle$ for different volume fractions c_1 of the reinforcement. As is seen, microdamages are responsible for the nonlinearity of the macrostress–macrostrain relationship, which is most pronounced at small values of c_1.

Figures 5 and 6 show (for (1.42) and (1.45), respectively) the porosity p_2 of the matrix as a function of the macrostrains $\langle \varepsilon_{11} \rangle$ and $\langle \varepsilon_{33} \rangle$ for different values of c_1. It can be seen that the behavior of the curves of $\langle \sigma_{11} \rangle / \mu_2$ versus $\langle \varepsilon_{11} \rangle$, $\langle \sigma_{33} \rangle / \mu_2$ versus $\langle \varepsilon_{33} \rangle$, and p_2 versus $\langle \varepsilon_{33} \rangle$ significantly depends on c_1, whereas c_1 has a weak effect on the curve of p_2 versus $\langle \varepsilon_{11} \rangle$.

1.4. Fibrous Composite. Consider a unidirectional fibrous material of stochastic structure with damages occurring in the matrix alone and being described by porosity p_2. Fibers are transversely isotropic and normal to the isotropy plane $x_1 x_2$. Denote the elastic moduli of fibers by $\lambda_{11}^1, \lambda_{12}^1, \lambda_{13}^1, \lambda_{33}^1$, and λ_{44}^1; the bulk and shear moduli of the undamaged portion of the matrix by K_2 and μ_2; and the volume fractions of fibers and porous matrix by c_1 and c_2, respectively. If the macrostrains $\langle \varepsilon_{jk} \rangle$ are given, then the macrostresses $\langle \sigma_{jk} \rangle$ are defined by (1.36), where the effective moduli λ_{pq}^* are determined from the following formulas [10, 34, 35, 37]:

$$\lambda_{11}^* + \lambda_{12}^* = c_1(\lambda_{11}^1 + \lambda_{12}^1) + 2c_2(\lambda_{2p} + \mu_{2p}) - \frac{c_1 c_2 (\lambda_{11}^1 + \lambda_{12}^1 - 2\lambda_{2p} - 2\mu_{2p})^2}{2c_1(\lambda_{2p} + \mu_{2p}) + c_2(\lambda_{11}^1 + \lambda_{12}^1) + 2m},$$

$$\lambda_{11}^* - \lambda_{12}^* = c_1(\lambda_{11}^1 - \lambda_{12}^1) + 2c_2\mu_{2p} - \frac{c_1 c_2 (\lambda_{11}^1 - \lambda_{12}^1 - 2\mu_{2p})^2}{2c_1\mu_{2p} + c_2(\lambda_{11}^1 - \lambda_{12}^1) + 2n},$$

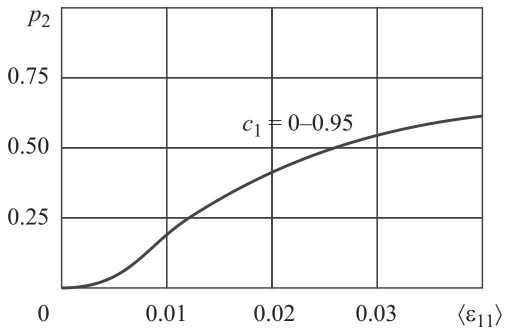

Fig. 5

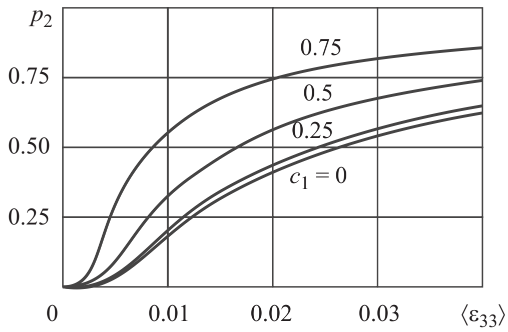

Fig. 6

$$\lambda_{13}^* = c_1\lambda_{13}^* + c_2\lambda_{2p} - \frac{c_1c_2(\lambda_{11}^1 + \lambda_{12}^1 - 2\lambda_{2p} - 2\mu_{2p})(\lambda_{13}^1 - \lambda_{2p})}{2c_1(\lambda_{2p} + \mu_{2p}) + c_2(\lambda_{11}^1 + \lambda_{12}^1) + 2m},$$

$$\lambda_{33}^* = c_1\lambda_{33}^* + c_2(\lambda_{2p} + 2\mu_{2p}) - \frac{2c_1c_2(\lambda_{13}^1 - \lambda_{2p})^2}{2c_1(\lambda_{2p} + \mu_{2p}) + c_2(\lambda_{11}^1 + \lambda_{12}^1) + 2m},$$

$$\lambda_{44}^* = c_1\lambda_{44}^1 + c_2\mu_{2p} - \frac{c_1c_2(\lambda_{44}^1 - \mu_{2p})^2}{c_1\mu_{2p} + c_2\lambda_{44}^1 + s}, \tag{1.48}$$

where

$$2m = c_1(\lambda_{11}^1 - \lambda_{12}^1) + 2c_2\mu_{2p}, \quad 2n = c_1(\lambda_{11}^1 + \lambda_{12}^1) + 2c_2(\lambda_{2p} + \mu_{2p}), \quad s = c_1\lambda_{44}^1 + 2c_2\mu_{2p} \tag{1.49}$$

if the matrix is stiffer than the fiber reinforcement and

$$2m = \left(\frac{c_1}{\lambda_{11}^1 - \lambda_{12}^1} + \frac{c_2}{2\mu_{2p}}\right)^{-1}, \quad 2n = \left(\frac{c_1}{\lambda_{11}^1 + \lambda_{12}^1} + \frac{c_2}{2(\lambda_{2p} + \mu_{2p})}\right)^{-1}, \quad s = \left(\frac{c_1}{\lambda_{44}^1} + \frac{c_2}{2\mu_{2p}}\right)^{-1} \tag{1.50}$$

if the reinforcement is stiffer than the matrix.

The effective moduli K_{2p} and μ_{2p} are defined by (1.17) ($i = 2$), according to [33].

A single microdamage occurs in the undamaged portion of the matrix in accordance with the Huber–Von Mises failure criterion (1.18) ($i = 2$). The one-point distribution function of k_2 may have the form of (1.19) or (1.20).

From the same considerations as in Sec. 1.2, we can write the equation of balance of damaged microvolumes in the matrix or its porosity [51, 55] in the form (1.21), where $\overline{\sigma}_{jk}^2$ and $\langle\sigma_{jk}^2\rangle$ are related by (1.40) ($i = 2$), which reduces the porosity balance equation (1.21) to the form (1.41) ($i = 2$), where $\langle\sigma_{jk}^2\rangle$ and $\langle\varepsilon_{jk}^2\rangle$ are related by

$$\langle\sigma_{jk}^2\rangle = \lambda_{2p}\langle\varepsilon_{rr}^2\rangle\delta_{jk} + 2\mu_{2p}\langle\varepsilon_{jk}^2\rangle, \tag{1.51}$$

and $\langle\varepsilon_{ij}^2\rangle$ are expressed in terms of macrostrains as follows [10, 34, 35, 37]:

$$\langle\varepsilon_{jk}^2\rangle = \frac{\lambda_{11}^* - \lambda_{12}^* - \lambda_{11}^1 + \lambda_{12}^1}{c_2(2\mu_{2p} - \lambda_{11}^1 + \lambda_{12}^1)}\langle\varepsilon_{jk}\rangle - \frac{1}{\Delta_2}\Big\{[(\lambda_{11}^* - \lambda_{11}^1)a_1 - (\lambda_{12}^* - \lambda_{12}^1)a_2 - (\lambda_{13}^* - \lambda_{13}^1)a_3]\langle\varepsilon_{rr}\rangle$$

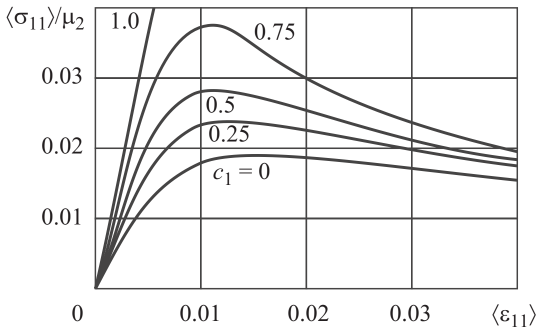

Fig. 7

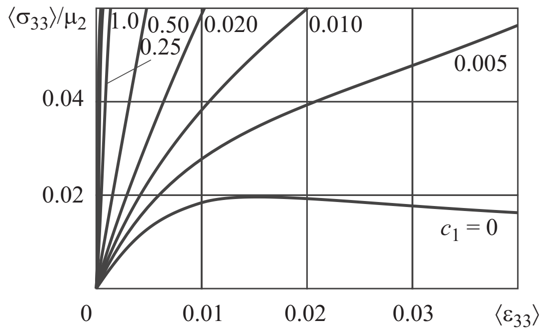

Fig. 8

$$+[(\lambda_{13}^{*}-\lambda_{13}^{1})(a_1-a_2)-(\lambda_{33}^{*}-\lambda_{33}^{1})a_3]\langle\varepsilon_{33}\rangle\Big\}\delta_{jk},$$

$$\langle\varepsilon_{33}^{2}\rangle=-\frac{1}{\Delta_2}\Big\{[(\lambda_{13}^{*}-\lambda_{13}^{1})a_4-(\lambda_{11}^{*}+\lambda_{12}^{*}-\lambda_{11}^{1}-\lambda_{12}^{1})a_3]\langle\varepsilon_{rr}\rangle+[(\lambda_{33}^{*}-\lambda_{33}^{1})a_4-2(\lambda_{13}^{*}-\lambda_{13}^{1})a_3]\langle\varepsilon_{33}\rangle\Big\},$$

$$\langle\varepsilon_{j3}^{2}\rangle=\frac{\lambda_{44}^{*}-\lambda_{44}^{1}}{c_2(\mu_{2p}-\lambda_{44}^{1})}\langle\varepsilon_{j3}\rangle\qquad(j,k,r=1,2),\tag{1.52}$$

where

$$\Delta_2=c_2(\lambda_{11}^{1}-\lambda_{12}^{1}-2\mu_{2p})\times[(\lambda_{11}^{1}+\lambda_{12}^{1}-2\lambda_{2p}-2\mu_{2p})(\lambda_{33}^{1}-\lambda_{2p}-2\mu_{2p})-2(\lambda_{13}^{1}-\lambda_{2p})^2],$$

$$a_1=(\lambda_{13}^{1}-\lambda_{2p})^2-(\lambda_{12}^{1}-\lambda_{2p})(\lambda_{33}^{1}-\lambda_{2p}-2\mu_{2p}),$$

$$a_2=(\lambda_{13}^{1}-\lambda_{2p})^2-(\lambda_{11}^{1}-\lambda_{2p}-2\mu_{2p})(\lambda_{33}^{1}-\lambda_{2p}-2\mu_{2p}),$$

$$a_3=(\lambda_{13}^{1}-\lambda_{2p})(\lambda_{11}^{1}-\lambda_{12}^{1}-2\mu_{2p}),$$

$$a_4=(\lambda_{11}^{1}+\lambda_{12}^{1}-2\lambda_{2p}-2\mu_{2p})(\lambda_{11}^{1}-\lambda_{12}^{1}-2\mu_{2p}),\tag{1.53}$$

and the effective moduli K_{2p}, λ_{2p}, and μ_{2p} are defined by (1.17).

The iterative algorithm (1.25)–(1.29) based on the secant method [4] and on (1.17), (1.48)–(1.51), (1.18), (1.19) (or (1.20)), (1.39), (1.40), (1.52), (1.53) was used to determine the volume fraction of microdamages in the matrix and the elastic characteristics of the composite and to plot stress–strain curves for a fibrous composite under loading of different types for the Weibull distribution (1.20). The components of the composite are high-modulus carbon fibers with volume fraction c_1 = 0, 0.25, 0.5, 0.75, 1.0 and the following elastic characteristics [20]:

$$E_1^1=8\text{ GPa},\quad E_3^1=226\text{ GPa},\quad \nu_{12}^1=0.3,\quad \nu_{13}^1=0.2,\quad G_{13}^1=60\text{ GPa},\tag{1.54}$$

and epoxy matrix with the characteristics (1.34) of the undamaged portion and (1.35); E_1^1 and E_3^1, ν_{12}^1 and ν_{13}^1, G_{12}^1 and G_{13}^1 are transverse and longitudinal Young's moduli, Poisson's ratios, and shear moduli of fibers related to λ_{11}^1, λ_{12}^1, λ_{13}^1, λ_{33}^1, and λ_{44}^1 by the formulas

$$\lambda_{11}^{1}+\lambda_{12}^{1}=E_1^1E_3^1\left[E_3^1\left(2-\frac{E_1^1}{2G_{12}^1}\right)-2E_1^1(\nu_{13}^1)^2\right]^{-1},\quad \lambda_{11}^{1}-\lambda_{12}^{1}=G_{12}^1,$$

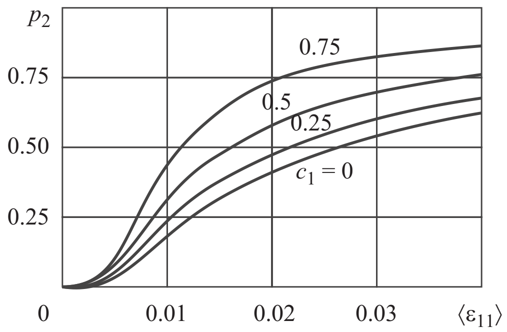

Fig. 9

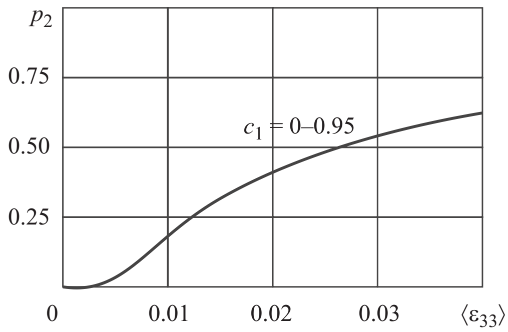

Fig. 10

$$\lambda_{13}^1 = \nu_{13}^1 (\lambda_{11}^1 + \lambda_{12}^1), \quad \lambda_{33}^1 = (\lambda_{11}^1 + \lambda_{12}^1) \frac{E_3^1}{E_1^1} \left(2 - \frac{E_1^1}{2G_{12}^1} \right), \quad \lambda_{44}^1 = G_{13}^1. \tag{1.55}$$

When the macroparameters (1.42) are given, the macrostress $\langle \sigma_{11} \rangle$ and the macrostrain $\langle \varepsilon_{11} \rangle$ are related by (1.43), according to (1.36), and Eq. (1.44) holds for (1.40).

When the macroparameters (1.45) are given, the macrostress $\langle \sigma_{33} \rangle$ and the macrostrain $\langle \varepsilon_{33} \rangle$ are related by (1.46), according to (1.36), and Eq. (1.47) holds for (1.40).

Figures 7 and 8 show (for (1.42) and (1.45), respectively) the macrostress $\langle \sigma_{11} \rangle / \mu_2$ as a function of the macrostrain $\langle \varepsilon_{11} \rangle$ and the macrostress $\langle \sigma_{33} \rangle / \mu_2$ as a function of the macrostrain $\langle \varepsilon_{33} \rangle$ for different volume fractions c_1 of fibers. As is seen, microdamages are responsible for the nonlinearity of the macrostress–macrostrain relationship, which is especially pronounced at small values of c_1.

Figures 9 and 10 show (for (1.42) and (1.45), respectively) the porosity p_2 of the matrix as a function of the macrostrain $\langle \varepsilon_{11} \rangle$ and macrostrain $\langle \varepsilon_{33} \rangle$ for different values of c_1. It can be seen that the behavior of the curves of $\langle \sigma_{11} \rangle / \mu_2$ versus $\langle \varepsilon_{11} \rangle$, $\langle \sigma_{33} \rangle / \mu_2$ versus $\langle \varepsilon_{33} \rangle$, and p_2 versus $\langle \varepsilon_{11} \rangle$ significantly depends on c1, whereas c_1 has a weak effect on the curve of p_2 versus $\langle \varepsilon_{33} \rangle$.

2. Modeling Microdamages by Pores Filled with Particles of a Damaged Material.

2.1. Homogeneous Material. The model outlined in Sec. 1.1 can easily be generalized by assuming that microdamages are pores filled with particles of a destroyed material that do not resist shear and uniform tension and resist uniform compression as the undamaged material does. Therefore, the shear modulus of the destroyed material in the pores is equal to zero and the bulk modulus is equal to zero if $\langle \bar{\sigma}_{rr}^2 \rangle \geq 0$ and to K if $\langle \bar{\sigma}_{rr}^2 \rangle < 0$, where $\langle \bar{\sigma}_{ij}^2 \rangle$ are the average stresses in the material filling the pores. When $\langle \bar{\sigma}_{rr}^2 \rangle \geq 0$, the effective moduli K^* and μ^* are defined by (1.2). If $\langle \bar{\sigma}_{rr}^2 \rangle < 0$, then, according to [36], we have

$$K^* = K, \quad \mu^* = \frac{[9K + 8\mu(1-p)]\mu(1-p)^2}{9K + 8\mu - (3K - 4\mu)p - 4\mu p^2}, \tag{2.1}$$

whence

$$\mu^* = \frac{[7 - 5\nu - 4(1-2\nu)p]\mu(1-p)^2}{7 - 5\nu - (1-\nu)p - 2(1-2\nu)p^2},$$

$$\nu^* = \frac{3\nu(7-5\nu) + (1-\nu)(17-37\nu)p - (1-2\nu)(17-19\nu)p^2 + 4(1-2\nu)^2 p^3}{3(7-5\nu) - 2(1-\nu)(10-17\nu)p + (1-2\nu)(11-25\nu)p^2 - 4(1-2\nu)^2 p^3}, \tag{2.2}$$

where ν is Poisson's ratio of the undamaged portion of the material.

Assuming that a single microdamage occurs in the undamaged portion of the material in accordance with the Schleicher–Nadai failure criterion [13], which accounts for the difference between the tensile and compressive ultimate loads,

$$I_{\bar{\sigma}} + a\bar{\sigma}_{rr} = k, \quad I_{\bar{\sigma}} = (\bar{\sigma}'_{ij}\bar{\sigma}'_{ij})^{1/2}, \tag{2.3}$$

where a is a deterministic constant, we arrive at the following porosity balance equation [37]:

$$p = p_0 + (1-p_0)F(I_{\bar{\sigma}} + a\bar{\sigma}_{rr}), \tag{2.4}$$

where $I_{\bar{\sigma}}$ is defined by (1.6), and $\bar{\sigma}_{rr}$ by

$$\bar{\sigma}_{rr} = \begin{cases} \dfrac{1}{1-p}\langle\sigma_{rr}\rangle, & \langle\sigma_{rr}\rangle \ge 0, \\ \langle\sigma_{rr}\rangle, & \langle\sigma_{rr}\rangle < 0. \end{cases} \tag{2.5}$$

Taking (1.5)–(1.7) and (2.5) into account, we reduce Eq. (2.4) to the form (1.11) for $\bar{\sigma}_{rr}^2 \ge 0$ and to the form

$$p = p_0 + (1-p_0)F\left(\frac{2\mu^*}{1-p}I_\varepsilon + 3aK\langle\varepsilon_{rr}\rangle\right) \tag{2.6}$$

for $\bar{\sigma}_{rr}^2 < 0$, where μ^* is defined by (2.1).

Equations (1.1), (1.2), (2.1), and (2.6) constitute a closed-form system that describes the coupled processes of statistically homogeneous deformation and damage of a material with microdamages modeled by pores filled with a destroyed material. Specifying macrostrains $\langle\varepsilon_{ij}\rangle$, we find the porosity p from the nonlinear equations (2.1) and (2.6). Then, substituting p into (1.1) and (2.1), we arrive at nonlinear relationships between the macrostresses $\langle\sigma_{ij}\rangle$ and the macrostrains $\langle\varepsilon_{ij}\rangle$. Since Eqs. (2.1) and (2.6) are nonlinear, their general solution can be found iteratively.

2.2. Particulate Composite. Let us generalize the damage model for particulate composites (Sec. 1.2) by assuming that microdamages occurring in its components under loading are pores filled with particles of a damaged material. We will consider the simplest case where these particles resist uniform compression as the undamaged material does and do not resist shear and uniform tension; i.e., the shear modulus of the damaged material in pores is equal to zero and its bulk modulus is equal to zero for $\bar{\sigma}_{rr}^{ip} \ge 0 (i=1,2)$ and to the bulk modulus of the undamaged material K_i $(i=1, 2)$ for $\bar{\sigma}_{rr}^{ip} < 0 (i=1,2)$, where $\bar{\sigma}_{jk}^{ip}$ are the stresses in the pores filled with particles of the damaged ith component. Then, according to Sec. 1.2, when $\bar{\sigma}_{rr}^{ip} \ge 0$ (the average stresses in filled pores of the ith component are tensile), the effective moduli of damaged inclusions, K_{1p}, μ_{1p}, and matrix, K_{2p}, μ_{2p}, are defined by formulas (1.17). When $\bar{\sigma}_{rr}^{ip} < 0$ (the stresses are compressive), we have [36]

$$K_{ip} = K_i, \quad \mu_{ip} = \frac{[9K_i + 8\mu_i(1-p_i)]\mu_i(1-p_i)^2}{9K_i + 8\mu_i - (3K_i + 4\mu_i)p_i - 4\mu_i p_i^2} \quad (i=1,2). \tag{2.7}$$

Assuming that a microdamage occurs in the undamaged portion of the ith component in accordance with the Schleicher–Nadai failure criterion [13]

$$I_{\bar{\sigma}}^i + a_i\bar{\sigma}_{rr}^i = k_i, \quad I_{\bar{\sigma}}^i = (\bar{\sigma}'^i_{ij}\bar{\sigma}'^i_{ij})^{1/2} \quad (i=1,2), \tag{2.8}$$

we arrive at the following porosity balance equation [51, 53]:

$$p_i = p_{0i} + (1-p_{0i})F_i(I_{\bar{\sigma}}^i + a_i\bar{\sigma}_{rr}^i), \tag{2.9}$$

where $I_{\bar{\sigma}}^2$ is defined by formula (1.39), and $\bar{\sigma}_{rr}^i$ is given by

$$\bar{\sigma}_{rr}^i = \begin{cases} \dfrac{1}{1-p_i}\langle\sigma_{rr}^i\rangle, & \langle\sigma_{rr}^i\rangle \ge 0, \\ \langle\sigma_{rr}^i\rangle, & \langle\sigma_{rr}^i\rangle < 0, \end{cases} \tag{2.10}$$

where $\langle \sigma_{rr}^i \rangle$ are the average stresses in the ith component.

Given macrostrains $\langle \varepsilon_{jk} \rangle$, we can use relations (2.12) and the following relationship between $\langle \sigma_{jk}^i \rangle$ and $\langle \varepsilon_{jk}^i \rangle$:

$$\langle \sigma_{jk}^i \rangle = \left(K_{ip} - \frac{2}{3} \mu_{ip} \right) \langle \varepsilon_{rr}^i \rangle \delta_{jk} + 2\mu_{ip} \langle \varepsilon_{jk}^i \rangle \tag{2.11}$$

to reduce the conditions $\langle \sigma_{rr}^i \rangle \geq 0$ and $\langle \sigma_{rr}^i \rangle < 0$ to the following form:

$$\langle \sigma_{rr}^i \rangle = 3(-1)^{i+1} K_{ip} \frac{(K^* - K_{(3-i)p})\langle \varepsilon_{rr} \rangle}{c_i (K_{1p} - K_{2p})} \geq 0 \tag{2.12}$$

$$\langle \sigma_{rr}^i \rangle = 3(-1)^{i+1} K_{ip} \frac{(K^* - K_{(3-i)p})\langle \varepsilon_{rr} \rangle}{c_i (K_{1p} - K_{2p})} < 0. \tag{2.13}$$

Considering relations (1.22), (1.23), and

$$\langle \varepsilon_{rr}^i \rangle = (-1)^{i+1} \frac{(K^* - K_{(3-i)p})\langle \varepsilon_{rr} \rangle}{c_i (K_{1p} - K_{2p})}, \tag{2.14}$$

we reduce the porosity balance equation (2.9) with (2.12) to the form (1.24), where the effective moduli of porous inclusions, K_{1p}, μ_{1p}, and matrix, K_{2p}, μ_{2p} are defined by (1.17). In view of (2.13), the porosity balance equation (2.9) can be rearranged into

$$p_i = p_{0i} + (1 - p_{0i}) F_i \left(\frac{2\mu_{ip}}{1 - p_i} I_\varepsilon^i + 3 a_i K_{ip} \langle \varepsilon_{rr}^i \rangle \right)$$

$$= p_{0i} + (1 - p_{0i}) F_i \left[\frac{2(-1)^{i+1} \mu_{ip} (\mu^* - \mu_{(3-k)p})}{(1 - p_i) c_i (\mu_{1p} - \mu_{2p})} I_{\langle \varepsilon \rangle} + 3(-1)^{i+1} a_i K_{ip} \frac{(K^* - K_{(3-i)p})\langle \varepsilon_{rr} \rangle}{c_i (K_{1p} - K_{2p})} \right], \tag{2.15}$$

where K_{1p}, μ_{1p} and K_{2p}, μ_{2p} are defined by (2.7).

The iterative algorithm (1.25)–(1.29) based on the secant method [12] and on (1.12)–(1.17), (1.19) (or (1.20)), (1.24), and (2.12) or (1.12)–(1.16), (2.7), (1.19) (or (1.20)), (2.15), and (2.13), which constitute systems of nonlinear algebraic equations for p_i, was used to determine the volume fraction of microdamages in the components and the elastic characteristics of the composite and to plot stress–strain curves of particulate composites with either empty pores or filled pores in the microdamaged matrix for the Weibull distribution (1.20) and the macroparameters (1.30). In this case, the macrostress $\langle \sigma_{11} \rangle$ and the macrostrain $\langle \varepsilon_{11} \rangle$ are related by (1.31), according to (1.1), and

$$I_{\langle \varepsilon \rangle} = \sqrt{\frac{3}{2}} \frac{K^* \langle \varepsilon_{11} \rangle}{K^* + 1/3\mu^*}, \quad \langle \varepsilon_{rr} \rangle = \frac{\mu^* \langle \varepsilon_{11} \rangle}{K^* + 1/3\mu^*} \tag{2.16}$$

in the porosity balance equation in the form (1.24), (2.12) or (2.15), (2.13).

Let

$$\frac{K_2}{K_1} = \frac{\mu_2}{\mu_1} = 0.1, \quad \nu_1 = \nu_2 = 0.3, \quad c_1 = 0, 0.25, 0.5, 0.75, 1.0, \tag{2.17}$$

where ν_1 and ν_2 are Poisson's ratios of the inclusions and the undamaged portion of the matrix, respectively, and

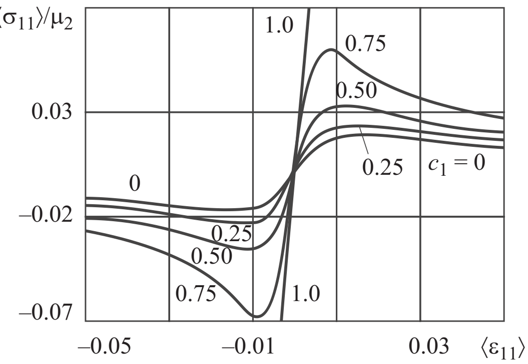

Fig. 11

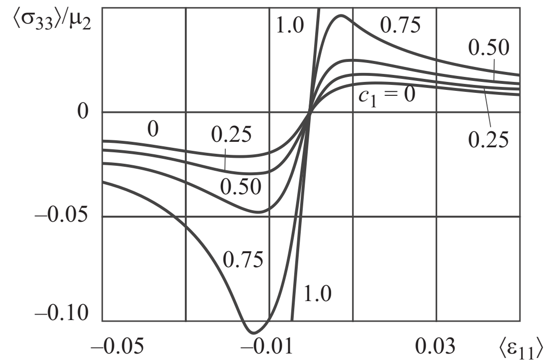

Fig. 12

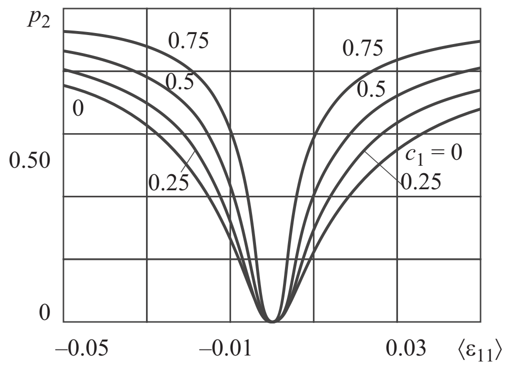

Fig. 13

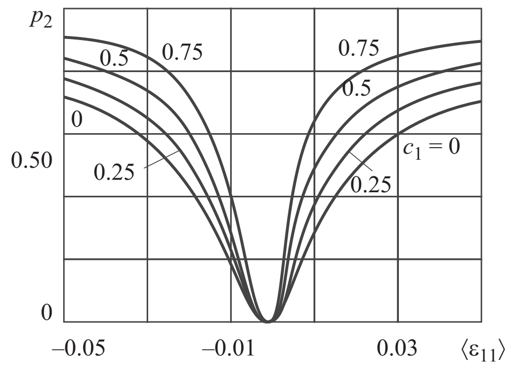

Fig. 14

$$p_{02} = 0, \quad \frac{k_{02}}{\mu_2} = 0.01, \quad m_2 = 1000, \quad \alpha_2 = 2, \quad a_2 = 0, 0.2. \tag{2.18}$$

Figures 11 and 12 show $\langle \sigma_{11} \rangle / \mu_2$ as a function of $\langle \varepsilon_{11} \rangle$ for $a_2 = 0$ and $a_2 = 0.2$, respectively. It is seen that the constant a_2, which characterizes the difference between the tensile and compressive strengths of the matrix, affects its elastic properties significantly. As a_2 increases, microdamages accumulate more intensively under tension (lower macrostress corresponds to fixed macrostrain) and more slowly under compression (larger macrostress corresponds to fixed macrostrain).

Figures 13 and 14 show the porosity p_2 of the matrix as a function of the macrostrain $\langle \varepsilon_{11} \rangle$ for $a_2 = 0$ and $a_2 = 0.2$, respectively. As is seen, the constant a_2 has a significant effect too.

2.3. Laminated Composite. Let us generalize the model of damaged laminated material with N components described in Sec. 1.3 by assuming that microdamages occurring under loading are pores filled with particles of a damaged material that resist triaxial compression as the undamaged material does and do not resist shear and triaxial tension. Then the shear modulus of the damaged material in the pores is equal to zero and the bulk modulus is equal to zero for $\overline{\sigma}_{rr}^{ip} \geq 0$ $(i = 1, ..., N)$ and to the bulk modulus K_i of the undamaged component for $\overline{\sigma}_{rr}^{ip} < 0$, where $\overline{\sigma}_{jk}^{ip}$ are the stresses in the pores filled with particles of the damaged ith component. Then, according to [33], when $\overline{\sigma}_{rr}^{ip} \geq 0$ (the average stresses in filled pores of the ith component are tensile), the effective moduli K_{ip} and μ_{ip} $(i = 1, ..., N)$ of the damaged component are defined by formulas (1.17). When $\overline{\sigma}_{rr}^{ip} < 0$ (the stresses are compressive), we have formulas (2.7) [36].

Assuming that a single microdamage occurs in the undamaged portion of the ith component in accordance with the Schleicher–Nadai failure criterion (2.8), we arrive at the porosity balance equation (2.9). Given macrostrains $\langle \varepsilon_{jk} \rangle$, we can use relations (1.41) to ascertain whether $\langle \sigma_{rr}^i \rangle \geq 0$ or $\langle \sigma_{rr}^i \rangle < 0$. Considering (1.10) and

$$I_{\sigma}^{i} = \frac{1}{1-p_i} I_{\langle\sigma\rangle}^{i}, \quad I_{\langle\sigma\rangle}^{i} = \left(\langle\sigma_{jk}^{i}\rangle'\langle\sigma_{jk}^{i}\rangle'\right)^{1/2}, \quad \overline{\sigma}_{rr}^{i} = \frac{\langle\sigma_{rr}^{i}\rangle}{1-p_i}, \tag{2.19}$$

we reduce the porosity balance equation (1.21) to the form (1.40) if $\langle\sigma_{rr}^{i}\rangle \geq 0$, where K_{ip} and μ_{ip} are given by (1.17). If $\langle\sigma_{rr}^{i}\rangle < 0$, the porosity balance equation (2.9) is reduced to

$$p_i = p_{0i} + (1-p_{0i})F_i\left(\frac{I_{\langle\sigma\rangle}^{i}}{1-p_i} + a_i\langle\sigma_{rr}^{i}\rangle\right), \tag{2.20}$$

where $\langle\sigma_{jk}^{i}\rangle$ and $\langle\varepsilon_{jk}\rangle$ are related by (1.41), and K_{ip} and μ_{ip} are given by (2.7).

The iterative algorithm (1.25)–(1.29) based on the secant method [4] and on (1.36), (1.37), (1.17), (1.19) (or (1.20)), (1.40), (1.41), and $\langle\sigma_{rr}^{i}\rangle \geq 0$ or (1.37), (1.38), (2.7), (1.19) (or (1.20)), (2.20), (1.41), and $\langle\sigma_{rr}^{i}\rangle < 0$, which are systems of nonlinear algebraic equations for p_i, was used to determine the volume fraction of microdamages in the components and the elastic characteristics of the composite and to study the deformation of two-component materials with microdamaged reinforcement for the Weibull distribution (1.20), two cases of loading (1.42) and (1.45), and the characteristics (2.17) and

$$p_{01} = 0, \quad k_{01}/\mu_2 = 0.01, \quad m_1 = 1000, \quad \alpha_1 = 2, \quad a_1 = 0, 0.2. \tag{2.21}$$

Given (1.42), the macrostress $\langle\sigma_{11}\rangle$ and the macrostrains $\langle\varepsilon_{11}\rangle$ are related by (1.43), according to (1.36), with equality (1.44) holding for (1.40) if $\langle\sigma_{rr}^{i}\rangle \geq 0$ or for (2.20) if $\langle\sigma_{rr}^{i}\rangle < 0$. Given (1.45), the macrostress $\langle\sigma_{33}\rangle$ and the macrostrain $\langle\varepsilon_{33}\rangle$ are related by (1.46), according to (1.36), with equality (1.47) holding for (1.40) if $\langle\sigma_{rr}^{i}\rangle \geq 0$ or for (2.20) if $\langle\sigma_{rr}^{i}\rangle < 0$.

A numerical analysis reveals that whether macrostresses and macrostrains are tensile or compressive hardly affects the behavior of $\langle\sigma_{11}\rangle/\mu_2$ as a function of $\langle\varepsilon_{11}\rangle$ and the behavior of $\langle\sigma_{33}\rangle/\mu_2$ as a function of $\langle\varepsilon_{33}\rangle$ and significantly affects the behavior of p_1 as a function of $\langle\varepsilon_{11}\rangle$ and $\langle\varepsilon_{33}\rangle$. In the former case, the dependence of the porosity p_1 on the macrostrain is quantitatively similar for any volume fraction c_1 of reinforcement because all layers undergo equal strains. In the latter case, stresses are equal and strains are different in physically dissimilar layers; hence, for different volume fractions c_1, the dependence of p_1 on $\langle\varepsilon_{33}\rangle$ behaves differently with changing macrostrain. The analysis also shows that the constant a_1, which characterizes the difference of tensile and compressive strengths, also affects substantially the elastic properties and porosity of the matrix.

2.4. Fibrous Composite. Let us generalize the model of damaged fibrous material described in Sec 1.4 by assuming that microdamages occurring in the matrix under loading are pores filled with particles of a damaged material that resist triaxial compression as the undamaged material does and do not resist shear and triaxial tension. Then the shear modulus of the damaged material is equal to zero and the bulk modulus is equal to zero if $\overline{\sigma}_{rr}^{2p} \geq 0$ and equal to the bulk modulus K_2 of the undamaged matrix if $\overline{\sigma}_{rr}^{2p} < 0$, where $\overline{\sigma}_{ij}^{2p}$ are the stresses in the pores filled with particles of the damaged matrix. Then, according to [33], when $\overline{\sigma}_{rr}^{2p} \geq 0$, the effective moduli K_{2p}, λ_{2p}, and μ_{2p} of the damaged matrix are defined by (1.17). When $\overline{\sigma}_{rr}^{2p} < 0$, they are calculated by formulas (2.7) [36].

Assuming that a single microdamage occurs in the undamaged portion of the matrix in accordance with the Schleicher–Nadai failure criterion (2.8) (i = 2), we arrive at the porosity balance equation (2.9) (i = 2), where I_{σ}^{2} is given by (1.39) (i = 2), and $\overline{\sigma}_{rr}^{2}$ by (2.10) (i = 2). Given the macrostrains $\langle\varepsilon_{ij}\rangle$, we can use relations (1.51)–(1.53) to ascertain whether $\overline{\sigma}_{rr}^{2p} \geq 0$ or $\overline{\sigma}_{rr}^{2p} < 0$. Considering relations (1.39) and (2.10) (i = 2), we can reduce the porosity balance equation (2.9) to the form (1.40) (i = 2) if $\overline{\sigma}_{rr}^{2p} \geq 0$, where K_{2p}, λ_{2p}, and μ_{2p} are given by (1.17) (i = 2), and to the form (2.20) (i = 2) if $\overline{\sigma}_{rr}^{2p} < 0$, where $\langle\sigma_{ij}^{2}\rangle$ and $\langle\varepsilon_{ij}\rangle$ are related by (1.51)–(1.53) and K_{2p}, λ_{2p}, and μ_{2p} are defined by (2.7) (i = 2).

The iterative algorithm (1.25)–(1.29) based on the secant method [12] and on (1.48)–(1.50), (1.17), (1.19) (or (1.20)), (1.40), (1.41), and $\langle\sigma_{rr}^{2}\rangle \geq 0$ or (1.48)–(1.50), (2.7), (1.19) (or (1.20)), (2.20), (1.41), and $\langle\sigma_{rr}^{2}\rangle < 0$, which are systems of

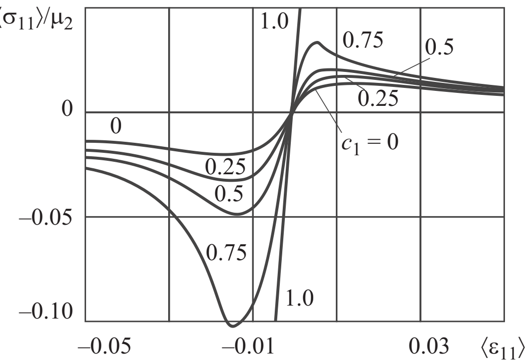

Fig. 15

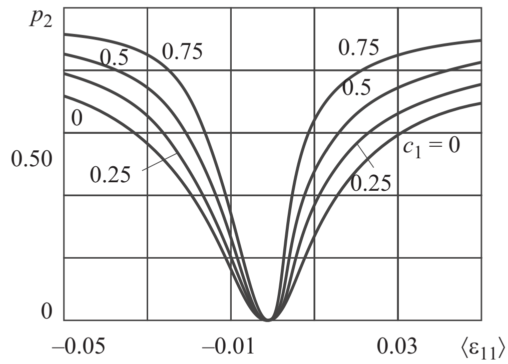

Fig. 16

nonlinear algebraic equations for p_2, was used to plot stress–strain curves for fibrous materials with microdamaged matrix for the Weibull distribution (1.20), macroparameters (1.42), (1.45), (2.18), and

$$\frac{E_1^1}{E_2} = \frac{G_{12}^1}{G_2} = 10, \quad \frac{E_3^1}{E_1^1} = 10, \quad \frac{G_{12}^1}{G_2} = 1, \quad \nu_{13}^1 = 0.2, \quad \nu_{13}^1 = \nu_2 = 0.3, \quad c_1 = 0, 0.25, 0.5, 0.75, 1.0, \tag{2.22}$$

where G_2 is the shear modulus of the undamaged portion of the matrix.

Given (1.42), the macrostress $\langle\sigma_{11}\rangle$ and the macrostrain $\langle\varepsilon_{11}\rangle$ are related by (1.43), according to (1.36), with equality (1.44) holding for (1.40) if $\langle\sigma_{rr}^i\rangle \geq 0$ or for (2.20) if $\langle\sigma_{rr}^i\rangle < 0$. Given (1.45), the macrostress $\langle\sigma_{33}\rangle$ and the macrostrain $\langle\varepsilon_{33}\rangle$ are related by (1.46), according to (1.36), with equality (1.47) holding for (1.40) if $\langle\sigma_{rr}^i\rangle \geq 0$ or for (2.20) if $\langle\sigma_{rr}^i\rangle < 0$.

Figure 15 and 16 show $\langle\sigma_{11}\rangle / \mu_2$ and p_2, respectively, as functions of $\langle\varepsilon_{11}\rangle$ for the macroparameters (1.42). Figures 17 and 18 show $\langle\sigma_{33}\rangle / \mu_2$ and p_2, respectively, as functions of $\langle\varepsilon_{33}\rangle$ for the macroparameters (1.45). It can be seen that the behavior of all the curves depends considerably on whether the macrostresses and macrostrains are tensile or compressive. The curves of $\langle\sigma_{11}\rangle / \mu_2$ versus $\langle\varepsilon_{11}\rangle$ for $c_1 < 1$ include two sections: linear ascending and nonlinear descending. Since in this case the strains in the matrix and fibers are different, the behavior of the curve of p_2 versus $\langle\varepsilon_{11}\rangle$ depends on the volume fraction c_1 of fibers. The curves of $\langle\sigma_{33}\rangle / \mu_2$ versus $\langle\varepsilon_{33}\rangle$ for $c_1 > 0$ are virtually linear and ascending, and the behavior of the curves of p_2 versus $\langle\varepsilon_{11}\rangle$ is hardly dependent on c_1. The analysis also shows that the constant a_2 strongly affects the elastic properties and porosity of the matrix with growth of macrostrains.

3. Short-Term Damage under Thermal Loading.

3.1. Homogeneous Material. Let us consider the simplest structural model of a damaged homogeneous material with dispersed microdamages modeled by randomly arranged quasispherical empty micropores. The macrostresses $\langle\sigma_{ij}\rangle$, macrostrains $\langle\varepsilon_{ij}\rangle$, and temperature θ of such a material with damage characterized by porosity p are related by

$$\langle\sigma_{ij}\rangle = (K^* - 2\mu^* / 3)\langle\varepsilon_{rr}\rangle\delta_{ij} + 2\mu^* \langle\varepsilon_{ij}\rangle - \beta^* \theta\delta_{ij}, \tag{3.1}$$

where the effective bulk and shear moduli K^* and μ^* are defined by formulas (1.2), and the thermal stress and strain coefficients β^* and α^* are expressed as follows, according to the theory of porous media [10, 34, 35, 37]:

$$\beta^* = \frac{4\mu\beta(1-p)^2}{4\mu + (3K - 4\mu)p}, \quad \alpha^* = \frac{\beta^*}{3K^*} = \frac{\beta}{3K} = \alpha, \tag{3.2}$$

where K, μ and β, α are the bulk and shear moduli and the thermal stress and strain coefficients of the undamaged portion of the material (skeleton).

In what follows, it will be convenient to use relations (1.3) and

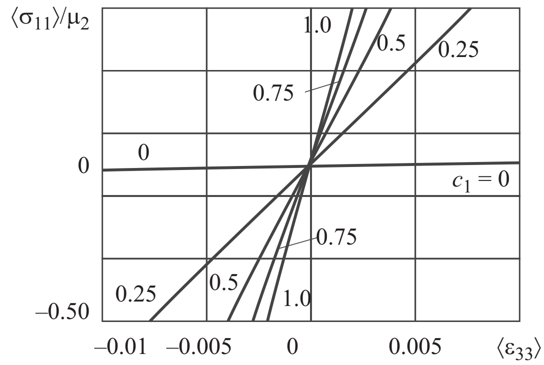

Fig. 17

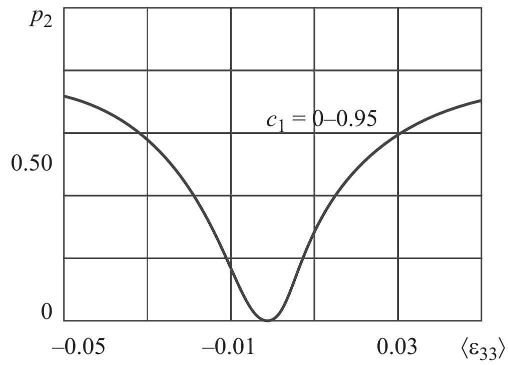

Fig. 18

$$\beta^* = \frac{2(1-2\nu)\beta(1-p)^2}{2(1-2\nu)-(1-5\nu)p}, \tag{3.3}$$

where ν is Poisson's ratio of the undamaged portion of the material.

Assuming that a single microdamage occurs in the undamaged portion of the material in accordance with the Schleicher–Nadai failure criterion (2.4) [13], where the average stresses $\overline{\sigma}_{ij}$ in the undamaged material are related to the macrostresses by

$$\overline{\sigma}_{ij} = \frac{1}{1-p}\langle\sigma_{ij}\rangle, \tag{3.4}$$

according to (3.1), we arrive at (1.6) and

$$\overline{\sigma}_{ij} = \frac{1}{1-p}\langle\sigma_{ij}\rangle = \frac{3}{1-p}(K^*\langle\varepsilon_{rr}\rangle - \beta^*\theta). \tag{3.5}$$

Thus, we can write the equation of balance of damaged microvolumes or porosity in the form (2.4). In view of (1.6) and (3.5), the porosity balance equation for given $\langle\varepsilon_{ij}\rangle$ and θ can be rearranged into the form

$$p = p_0 + (1-p_0)F\left[\frac{2\mu^*}{1-p}I_\varepsilon + \frac{3a}{1-p}(K^*\langle\varepsilon_{rr}\rangle - \beta^*\theta)\right]. \tag{3.6}$$

Equations (3.1), (1.2), (3.2), and (3.6) constitute a closed-form system describing the coupled processes of statistically homogeneous deformation and damage of a material under mechanical and thermal loading. Given the macrostrains $\langle\varepsilon_{ij}\rangle$ and temperature θ, we can find the porosity p from the nonlinear equations (1.2), (3.2), and (3.6). Then, substituting p into (3.1), (1.2), and (3.2), we arrive at a nonlinear relationship among $\langle\sigma_{ij}\rangle$, $\langle\varepsilon_{ij}\rangle$, and θ. Since Eqs. (1.2), (3.2), and (3.6) are nonlinear, their general solution can be found iteratively.

The above model can be generalized by assuming that microdamages are pores filled with particles of a damaged material that resist triaxial compression as the undamaged material does and do not resist shear and triaxial tension. Then the shear modulus of the damaged material filling pores is equal to zero and its bulk modulus is equal to zero when $\langle\overline{\sigma}^2_{rr}\rangle \geq 0$ and is equal to K when $\langle\overline{\sigma}^2_{rr}\rangle < 0$, where $\langle\overline{\sigma}^2_{rr}\rangle$ are the average stresses in the material filling the pores. For $\langle\overline{\sigma}^2_{rr}\rangle \geq 0$, the effective moduli K^* and μ^* and the coefficients β^* and α^* are defined by (1.2) and (3.2). For $\langle\overline{\sigma}^2_{rr}\rangle < 0$, according to [6], we have (2.1) and

$$\beta^* = \beta, \qquad \alpha^* = \alpha. \tag{3.7}$$

Assuming that a single microdamage occurs in the undamaged portion in accordance with the Schleicher–Nadai failure criterion (2.3), we arrive at the porosity balance equation (2.4), where $I_{\overline{\sigma}}$ is defined by (1.6) and $\langle\overline{\sigma}_{rr}\rangle$ by (2.5).

Considering relations (1.6), (2.1), (2.5), (3.5), and (3.7), we reduce the porosity balance equation (2.4) to the form (3.6) when $\langle\sigma_{rr}\rangle \geq 0$ and to the form

$$p = p_0 + (1 - p_0)F\left[\frac{2\mu^*}{1-p} I_\varepsilon + \frac{3a}{1-p}(K\langle\varepsilon_{rr}\rangle - \beta\theta)\right] \tag{3.8}$$

when $\langle\sigma_{rr}\rangle < 0$, where μ^* is defined by (1.3) and (2.1).

3.2. Particulate Composite. We will model dispersed microdamages in the components of a particulate composite by randomly arranged quasispherical empty micropores. Denote the porosities and volume fractions of the matrix and inclusions by p_1, c_1 and p_2, c_2, respectively; and their bulk and shear moduli and thermal stress and strain coefficients by $K_1, \mu_1, \beta_1, \alpha_1$ and $K_2, \mu_2, \beta_2, \alpha_2$. The macrostrains $\langle\varepsilon_{jk}\rangle$, macrostresses $\langle\sigma_{jk}\rangle$, and temperature θ are related by (3.1), where the effective constants K^*, μ^*, β^*, and α^* are expressed, according to [10, 34, 35, 37], in terms of the analogous constants of porous inclusions and porous matrix, $K_{1p}, \mu_{1p}, \beta_{1p}, \alpha_{1p}$ and $K_{2p}, \mu_{2p}, \beta_{2p}, \alpha_{2p}$, by formulas (1.13)–(1.15) and

$$\beta^* = c_1\beta_{1p} + c_2\beta_{2p} - \frac{c_1c_2(K_{1p} - K_{2p})(\beta_{1p} - \beta_{2p})}{c_1K_{2p} + c_2K_{1p} + n_c}, \quad \alpha^* = \frac{\beta^*}{3K^*}. \tag{3.9}$$

The effective moduli and thermal coefficients of the porous matrix and inclusions are defined by (1.17), according to [33], and by

$$\beta_{ip} = \frac{4\beta_i\mu_i(1-p_i)^2}{4\mu_i + (3K_i - 4\mu_i)p_i}, \quad \alpha_{ip} = \frac{\beta_{ip}}{3K_{ip}} = \frac{\beta_i}{3K_i} \quad (i = 1, 2). \tag{3.10}$$

Assuming that a single microdamage occurs in the undamaged portion of the ith component in accordance with the Schleicher–Nadai failure criterion (2.8), we can write the equation of balance of damaged microvolumes in the ith component or its porosity in the form (2.9), where equalities (1.22) and (1.23) hold and

$$\bar{\sigma}_{rr}^i = 3\frac{K_{ip}\langle\varepsilon_{rr}^i\rangle - \beta_{ip}\theta}{1-p_i},$$

$$\langle\varepsilon_{rr}^i\rangle = (-1)^{i+1}\frac{(K^* - K_{(3-k)p})\langle\varepsilon_{rr}\rangle - (\beta^* - c_1\beta - c_2\beta_{2p})\theta}{c_k(K_{1p} - K_{2p})}. \tag{3.11}$$

Taking relations (1.13)–(1.15), (1.17), (3.9)–(3.11) into account, we reduce the porosity balance equation (2.9) to the form

$$p_i = p_{0i} + (1 - p_{0i})F_i\left[\frac{2\mu_{ip}}{1-p_i} I_\varepsilon^i + \frac{3a_i}{1-p_i}(K_{ip}\langle\varepsilon_{rr}^i\rangle - \beta_{ip}\theta)\right]$$

$$= p_{0i} + (1 - p_{0i})F_i\left\{(-1)^{i+1}\frac{2\mu_{ip}\left(\mu^* - \mu_{(3-i)p}\right)}{(1-p_i)\,c_i\left(\mu_{1p} - \mu_{2p}\right)} I_{\langle\varepsilon\rangle}\right.$$

$$\left. + \frac{3a_i}{1-p_i}\left[(-1)^{i+1}K_{ip}\frac{\left(K^* - K_{(3-i)p}\right)\langle\varepsilon_{rr}\rangle - \left(\beta^* - c_1\beta_{1p} - c_2\beta_{2p}\right)\theta}{c_i\left(K_{1p} - K_{2p}\right)} - \beta_{ip}\theta\right]\right\}, \tag{3.12}$$

where the effective moduli and thermal coefficients of the porous inclusions and matrix, $K_{1p}, \mu_{1p}, \beta_{1p}$ and $K_{2p}, \mu_{2p}, \beta_{2p}$, are defined by (1.17) and (3.10).

Let us generalize the model of damaged particulate composite by assuming that microdamages are pores filled with particles of a damaged material that, in the simplest case, resist triaxial compression as the undamaged material does and do not resist shear and triaxial tension. Then the shear modulus of the damaged material filling pores is equal to zero and its bulk modulus is equal to zero when $\overline{\sigma}_{rr}^{ip} \geq 0 \, (i = 1, 2)$ and is equal to the bulk modulus K_i of the undamaged component $(i = 1, 2)$ when $\overline{\sigma}_{rr}^{ip} < 0 \, (i = 1, 2)$, where $\overline{\sigma}_{jk}^{ip}$ are the stresses in filled pores of the ith component. Then, according to Sec. 1, when $\overline{\sigma}_{rr}^{ip} \geq 0$ (the average bulk stresses in the particles filling pores of the ith component are tensile), the effective moduli and thermal coefficients of the porous inclusions and matrix, $K_{1p}, \mu_{1p}, \beta_{1p}$ and $K_{2p}, \mu_{2p}, \beta_{2p}$, are defined by (1.17). When $\overline{\sigma}_{rr}^{ip} < 0$ (the stresses are compressive), we have (2.7) and

$$\beta_{ip} = \beta_i, \quad \alpha_{ip} = \alpha_i \quad (i = 1, 2). \tag{3.13}$$

Assuming that a single microdamage occurs in the undamaged portion of the ith component in accordance with the Schleicher–Nadai failure criterion (2.8), we arrive at the porosity balance equation (2.9), where I_{σ}^{i} is defined by formula (1.22), (1.23) and $\overline{\sigma}_{rr}^{i}$ by (2.10).

We use the relationship among $\langle \sigma_{jk}^{i} \rangle$, $\langle \varepsilon_{jk}^{i} \rangle$, and θ

$$\langle \sigma_{jk}^{i} \rangle = \left(K_{ip} - \frac{2}{3}\mu_{ip} \right) \langle \varepsilon_{rr}^{i} \rangle \delta_{jk} + 2\mu_{ip} \langle \varepsilon_{jk}^{i} \rangle - \beta_{ip} \theta \delta_{jk} \tag{3.14}$$

and relations (3.11) to reduce the conditions $\langle \sigma_{rr}^{i} \rangle \geq 0$ and $\langle \sigma_{rr}^{i} \rangle < 0$ to the form

$$\langle \sigma_{rr}^{i} \rangle = 3(-1)^{i+1} K_{ip} \frac{(K^{*} - K_{(3-i)p}) \langle \varepsilon_{rr} \rangle - (\beta^{*} - c_1 \beta_{1p} - c_2 \beta_{2p}) \theta}{c_i (K_{1p} - K_{2p})} - 3\beta_{ip} \theta \geq 0 \tag{3.15}$$

$$\langle \sigma_{rr}^{i} \rangle = 3(-1)^{i+1} K_{ip} \frac{(K^{*} - K_{(3-i)p}) \langle \varepsilon_{rr} \rangle - (\beta^{*} - c_1 \beta_{1p} - c_2 \beta_{2p}) \theta}{c_i (K_{1p} - K_{2p})} - 3\beta_{ip} \theta < 0. \tag{3.16}$$

In view of (1.22), (1.23), and (2.14), the porosity balance equation (2.9) reduces to the form (3.12) if (3.15) holds, where $K_{1p}, \mu_{1p}, \beta_{1p}$ and $K_{2p}, \mu_{2p}, \beta_{2p}$ are defined by (2.17) and (3.10), and to the following form if (3.16) holds:

$$p_i = p_{0i} + (1 - p_{0i}) F_i \left[\frac{2\mu_{ip}}{1 - p_i} I_{\varepsilon}^{i} + 3a_i (K_{ip} \langle \varepsilon_{rr}^{i} \rangle - \beta_{ip} \theta) \right]$$

$$= p_{0i} + (1 - p_{0i}) F_i \left\{ (-1)^{i+1} \frac{2\mu_{ip} (\mu^{*} - \mu_{(3-i)p})}{(1 - p_i) c_i (\mu_{1p} - \mu_{2p})} I_{\langle \varepsilon \rangle} \right.$$

$$\left. + 3a_i \left[(-1)^{i+1} K_{ip} \frac{(K^{*} - K_{(3-i)p}) \langle \varepsilon_{rr} \rangle - (\beta^{*} - c_1 \beta_{1p} - c_2 \beta_{2p}) \theta}{c_i (K_{1p} - K_{2p})} - \beta_{ip} \theta \right] \right\}, \tag{3.17}$$

where $K_{1p}, \mu_{1p}, \beta_{1p}$ and $K_{2p}, \mu_{2p}, \beta_{2p}$ are defined by (2.7) and (3.13).

The iterative algorithm (1.25)–(1.29) based on the secant method [12] and on (1.13)–(1.17), (3.9), (3.10), (1.19) (or (1.20)), (3.12), and (3.15) or (1.13)–(1.16), (3.9), (2.7), (3.13), (1.19) (or (1.20)), (3.17), and (3.16), which are systems of nonlinear algebraic equations for p_i, was used to plot stress–strain curves for particulate composites with microdamaged matrix

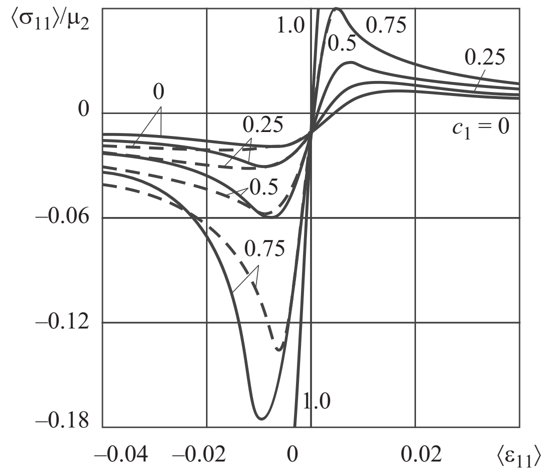

Fig. 19

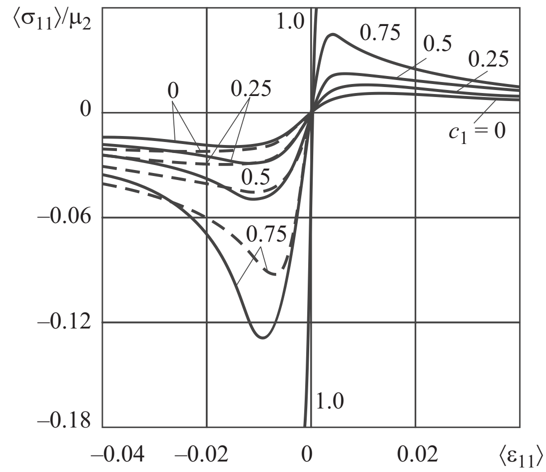

Fig. 20

for the Weibull distribution (1.20), macroparameters (1.30), and cases of empty and filled pores. According to (3.8), the macrostress $\langle\sigma_{11}\rangle$, macrostrain $\langle\varepsilon_{11}\rangle$, and temperature θ are related by

$$\langle\sigma_{11}\rangle = \frac{\mu^*}{K^* + 1/3\mu^*}(3K^*\langle\varepsilon_{11}\rangle - \beta^*\theta). \tag{3.18}$$

In (3.12), (3.15) and (3.17), (3.16), we have

$$I_{\langle\varepsilon\rangle} = \sqrt{\frac{2}{3}}\frac{\left|3K^*\langle\varepsilon_{11}\rangle - \beta^*\theta\right|}{2(K^* + 1/3\mu^*)}, \quad \langle\varepsilon_{rr}\rangle = \frac{\mu^*\langle\varepsilon_{11}\rangle + \beta^*\theta}{K^* + 1/3\mu^*}, \tag{3.19}$$

which is equivalent to (3.18).

The material of inclusions is aluminoborosilicate glass with the elastic characteristics and volume fraction (1.33) and the following thermal strain coefficient [10]:

$$\alpha_1 = 4.9\cdot 10^{-6}\ ^\circ\mathrm{C}^{-1}. \tag{3.20}$$

The material of the matrix is epoxy resin with the elastic characteristics of the undamaged portion (1.34) and the following thermal strain coefficient [20]:

$$\alpha_2 = 45\cdot 10^{-6}\ ^\circ\mathrm{C}^{-1}, \tag{3.21}$$

and parameter values (1.35).

Figures 19 and 20 show $\langle\sigma_{11}\rangle/\mu_2$ as a function of $\langle\varepsilon_{11}\rangle$ in the cases of tension and compression for $\alpha_2\theta = 0$ and $\alpha_2\theta = 0.0045$, respectively. In the case of compression, the solid lines correspond to pores filled with particles of a damaged material and the dashed lines to empty pores. As can be seen, damage sets in at lower macrostrain when pores are empty. The temperature has a significant effect on the stress–strain curves: microdamages begin to appear under lower compressive macrostrains and higher tensile macrostrains.

Figures 21 and 22 show p_2 as a function of $\langle\varepsilon_{11}\rangle$ for $\alpha_2\theta = 0$ and $\alpha_2\theta = 0.0045$, respectively. Comparing these curves with those that disregard the thermal effect reveals [46, 53, 57] that the temperature θ also has a significant influence on the behavior of the curve of porosity versus $\langle\varepsilon_{11}\rangle$.

Let us now consider the coupled processes of deformation and microdamage induced by thermal loading alone:

$$\langle\sigma_{11}\rangle = \langle\sigma_{22}\rangle = \langle\sigma_{33}\rangle = 0. \tag{3.22}$$

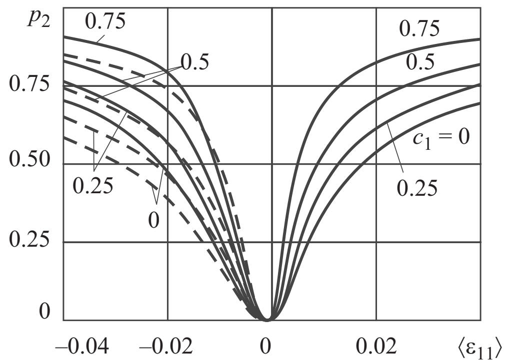

Fig. 21

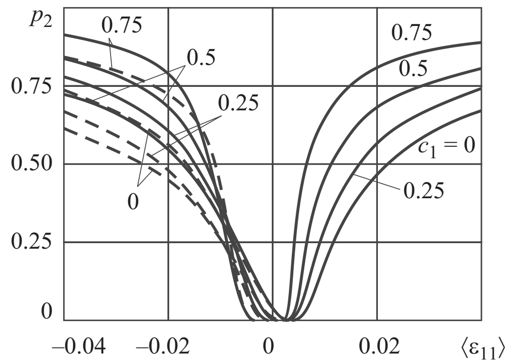

Fig. 22

In this case, the bulk macrostrain $\langle\varepsilon_{rr}\rangle$ and the temperature θ are related linearly by

$$\langle\varepsilon_{rr}\rangle = \frac{\beta^*}{K^*}\theta = 3\alpha^*\theta. \tag{3.23}$$

Assuming that no damage occurs under triaxial compression and considering that $I_{\langle\varepsilon\rangle}=0$ if (3.22), we reduce the porosity balance equation (3.12) to the form

$$p_i = p_{0i} + F\left[\frac{3a_i}{1-p_i}\frac{K_{1p}K_{2p}(\alpha^* - c_1\alpha_{1p} - c_2\alpha_{2p})}{(-1)^i c_i (K_{1p} - K_{2p})}\theta\right]. \tag{3.24}$$

According to (3.15) and (3.23), the bulk stresses in the components are defined by

$$\langle\sigma_{rr}^i\rangle = 3\frac{K_{1p}K_{2p}(\alpha^* - c_1\alpha_{1p} - c_2\alpha_{2p})}{(-1)^i c_i (K_{1p} - K_{2p})}\theta. \tag{3.25}$$

As can be seen, thermal loading can cause microdamage even in the absence of macrostresses because the coefficients of linear thermal expansion in the components are different and, thereby, one component is under compression and the other under tension. As a result, microdamages occur in the latter component.

Figure 23 shows the porosity p_2 of the matrix as a function of the thermal strain $\alpha_2\theta$ for (3.22) (no mechanical load).

3.3. Laminated Composite. Let us consider a laminated material with N isotropic components and dispersed microdamages modeled by empty pores. The bulk and shear moduli and the thermal stress and strain coefficients of the undamaged portion of the ith a component are denoted by $K_i, \mu_i, \beta_i, \alpha_i$; the porosity by p_i $(i=1,\dots,N)$; and the volume fraction of the porous ith component by c_i. Given the macrostrains $\langle\varepsilon_{jk}\rangle$ and temperature θ, the macrostresses $\langle\sigma_{jk}\rangle$ are expressed as

$$\langle\sigma_{jk}\rangle = (\lambda_{11}^* - \lambda_{12}^*)\langle\varepsilon_{jk}\rangle + (\lambda_{12}^*\langle\varepsilon_{rr}\rangle + \lambda_{13}^*\langle\varepsilon_{33}\rangle - \beta_1^*\theta)\delta_{jk},$$

$$\langle\sigma_{33}\rangle = \lambda_{13}^*\langle\varepsilon_{rr}\rangle + \lambda_{33}^*\langle\varepsilon_{33}\rangle - \beta_3^*\theta, \quad \langle\sigma_{j3}\rangle = 2\lambda_{44}^*\langle\varepsilon_{j3}\rangle \quad (j,k,r=1,2), \tag{3.26}$$

where the effective elastic moduli $\lambda_{11}^*, \lambda_{12}^*, \lambda_{13}^*, \lambda_{33}^*$, and λ_{44}^* are defined by (1.37) and the thermal stress and strain coefficients β_1^*, β_3^*, and α_1^*, α_3^* are determined [10, 34, 35, 37] in terms of the analogous moduli and coefficients of the porous components $\lambda_{ip}, \mu_{ip}, \beta_{ip}$ $(i=1,\dots,N)$:

$$\beta_1^* = \left\langle\frac{1}{\lambda_p + 2\mu_p}\right\rangle^{-1}\left\langle\frac{\lambda_p}{\lambda_p + 2\mu_p}\right\rangle\left\langle\frac{\beta_p}{\lambda_p + 2\mu_p}\right\rangle + 2\left\langle\frac{\beta_p\mu_p}{\lambda_p + 2\mu_p}\right\rangle,$$

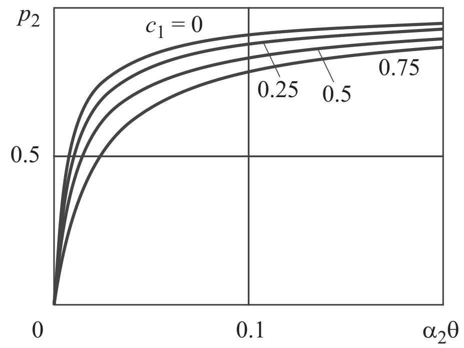

Fig. 23

$$\beta_3^* = \left\langle \frac{1}{\lambda_p + 2\mu_p} \right\rangle^{-1} \left\langle \frac{\beta_p}{\lambda_p + 2\mu_p} \right\rangle \qquad (\langle f^* \rangle = \sum_{i=1}^{N} c_i f_i^*),$$

$$\alpha_1^* = \frac{\lambda_{33}^* \beta_1^* - \lambda_{13}^* \beta_3^*}{(\lambda_{11}^* + \lambda_{12}^*)\lambda_{33}^* - 2(\lambda_{13}^*)^2}, \qquad \alpha_3^* = \frac{(\lambda_{11}^* + \lambda_{12}^*)\beta_3^* - 2\lambda_{13}^* \beta_1^*}{(\lambda_{11}^* + \lambda_{12}^*)\lambda_{33}^* - 2(\lambda_{13}^*)^2}. \tag{3.27}$$

If dispersed microdamages are modeled by randomly arranged quasispherical empty micropores, the effective moduli and thermal coefficients of the porous ith component, $K_{ip}, \lambda_{ip}, \mu_{ip}, \beta_{ip}, \alpha_{ip}$ $(\lambda_{ip} = K_{ip} - 2\mu_{ip}/3)$ $(i = 1, \ldots, N)$ are defined by (1.17) and (3.10).

Assuming that a single microdamage occurs in the undamaged portion of the ith component in accordance with the Schleicher–Nadai failure criterion (2.8) (i = 1, ..., N) and reasoning in the same way as in the cases of homogeneous or particulate composites, we arrive at the porosity balance equation in the form (2.9) (i = 1, ..., N), which in view of (1.39) and

$$\langle \bar{\sigma}_{jk}^i \rangle = \frac{1}{1 - p_i} \langle \sigma_{jk}^i \rangle \tag{3.28}$$

reduces to

$$p_i = p_{0i} + (1 - p_{0i}) F_i \left(\frac{I_{\langle\sigma\rangle}^i}{1 - p_i} + a_i \frac{\langle \sigma_{rr}^i \rangle}{1 - p_i} \right), \tag{3.29}$$

where $\langle \sigma_{jk}^i \rangle$, $\langle \varepsilon_{jk} \rangle$, and θ are related by the following formulas [10, 34, 35, 37]:

$$\langle \sigma_{jk}^i \rangle = 2\mu_{ip} \langle \varepsilon_{jk} \rangle + \frac{\lambda_{ip}}{\lambda_{ip} + 2\mu_{ip}} \left\langle \frac{1}{\lambda_p + 2\mu_p} \right\rangle^{-1} \left(\left\langle \frac{\lambda_p}{\lambda_p + 2\mu_p} \right\rangle + 2\mu_{ip} \left\langle \frac{1}{\lambda_p + 2\mu_p} \right\rangle \right) \langle \varepsilon_{rr} \rangle \delta_{jk}$$

$$+ \frac{\lambda_{ip}}{\lambda_{ip} + 2\mu_{ip}} \left\langle \frac{1}{\lambda_p + 2\mu_p} \right\rangle^{-1} \langle \varepsilon_{33} \rangle \delta_{jk} - \frac{1}{\lambda_{ip} + 2\mu_{ip}} \left\langle \frac{1}{\lambda_p + 2\mu_p} \right\rangle^{-1}$$

$$\times \left(\lambda_{ip} \left\langle \frac{\beta_p}{\lambda_p + 2\mu_p} \right\rangle + 2\mu_{ip} \beta_{ip} \left\langle \frac{1}{\lambda_p + 2\mu_p} \right\rangle \right) \theta \delta_{jk},$$

$$\langle \sigma_{33}^i \rangle = \left\langle \frac{1}{\lambda_p + 2\mu_p} \right\rangle^{-1} \left(\left\langle \frac{\lambda_p}{\lambda_p + 2\mu_p} \right\rangle \langle \varepsilon_{rr} \rangle + \langle \varepsilon_{33} \rangle - \left\langle \frac{\beta_p}{\lambda_p + 2\mu_p} \right\rangle \theta \right),$$

$$\langle \sigma^i_{j3} \rangle = 2\left\langle \frac{1}{\mu_p} \right\rangle^{-1} \langle \varepsilon_{j3} \rangle \quad (j,k,r = 1,2; \quad i = 1,\dots,N), \tag{3.30}$$

and $K_{ip}, \lambda_{ip}, \mu_{ip}$, and β_{ip} are defined by (1.17) and (3.10).

Let us generalize the above model by assuming that microdamages are pores filled with particles of a damaged material resisting deformation. Then, according to Sec. 1, when $\overline{\sigma}^{ip}_{rr} \geq 0$ (the average bulk stresses in the pores of the ith component are tensile), the effective moduli and thermal coefficients of the porous components, $K_{ip}, \lambda_{ip}, \mu_{ip}, \beta_{ip}$ $(i = 1,\dots,N)$, are defined by (1.17) and (3.10). When $\overline{\sigma}^{ip}_{rr} < 0$ (the stresses are compressive), according to Sec. 2, these moduli and coefficients are defined by (2.7) and (3.13).

Assuming that a single microdamage occurs in the undamaged portion of the ith component in accordance with the Schleicher–Nadai failure criterion (2.8), we arrive at the porosity balance equation in the form (2.9) (i = 1, ..., N), where $I^i_{\overline{\sigma}}$ is defined by (1.39) and $\overline{\sigma}^i_{rr}$ by (2.10).

Given $\langle \varepsilon_{jk} \rangle$ and θ in (3.30), we can ascertain whether $\langle \sigma^i_{rr} \rangle \geq 0$ or $\langle \sigma^i_{rr} \rangle < 0$. In view of (1.39) and (2.10), the porosity balance equation (2.9) reduces to the form (3.30) if $\langle \sigma^i_{rr} \rangle \geq 0$, where $K_{ip}, \lambda_{ip}, \mu_{ip}, \beta_{ip}$ are defined by (1.17) and (3.10), and to the following form if $\langle \sigma^i_{rr} \rangle < 0$:

$$p_i = p_{0i} + (1 - p_{0i}) F_i \left(\frac{I^i_{\langle\sigma\rangle}}{1 - p_i} + a_i \langle \sigma^i_{rr} \rangle \right), \tag{3.31}$$

where $\langle \sigma^i_{jk} \rangle$, $\langle \varepsilon_{jk} \rangle$, and θ are related by (3.31), and $K_{ip}, \lambda_{ip}, \mu_{ip}$, and β_{ip} are given by (2.7) and (3.13).

The iterative algorithm (1.25)–(1.29) based on the secant method [4] and on (1.37), (1.38), (3.27), (1.17), (3.10), (1.19) (or (1.20)), (3.30), (3.29), and $\langle \sigma^i_{rr} \rangle \geq 0$ or (1.37), (1.38), (3.27), (2.7), (3.13), (1.19) (or (1.20)), (3.30), (3.31), and $\langle \sigma^i_{rr} \rangle < 0$, which are systems of nonlinear algebraic equations for p_i, was used to determine the volume fraction of microdamages in the components and the elastic characteristics of the composite and to study the deformation of a laminated two-component composite with microdamages in the reinforcement for the Weibull distribution (1.20), different cases of loading, and the cases of empty and filled pores. The components are aluminoborosilicate glass with the characteristics and volume fraction (1.33), (3.20) and epoxy resin with characteristics (1.34), (3.21), (1.35), and $\alpha_1\theta = 0.00094$.

Given (1.42), according to (3.26), the macrostress $\langle \sigma_{11} \rangle$, macrostrain $\langle \varepsilon_{11} \rangle$, and temperature θ are related by

$$\langle \sigma_{11} \rangle = \frac{\lambda^*_{11} - \lambda^*_{12}}{\lambda^*_{11}\lambda^*_{33} - (\lambda^*_{13})^2} \{[(\lambda^*_{11} + \lambda^*_{12})\lambda^*_{33} - 2(\lambda^*_{13})^2] \langle \varepsilon_{11} \rangle - (\lambda^*_{33}\beta^*_1 - \lambda^*_{13}\beta^*_3)\theta\} \tag{3.32}$$

and

$$\langle \varepsilon_{22} \rangle = \frac{[(\lambda^*_{13})^2 - \lambda^*_{12}\lambda^*_{33}] \langle \varepsilon_{11} \rangle - (\lambda^*_{13}\beta^*_3 - \lambda^*_{33}\beta^*_1)\theta}{\lambda^*_{11}\lambda^*_{33} - (\lambda^*_{13})^2},$$

$$\langle \varepsilon_{33} \rangle = \frac{[(\lambda^*_{12} - \lambda^*_{11})\lambda^*_{13}] \langle \varepsilon_{11} \rangle - (\lambda^*_{13}\beta^*_1 - \lambda^*_{11}\beta^*_3)\theta}{\lambda^*_{11}\lambda^*_{33} - (\lambda^*_{13})^2} \tag{3.33}$$

in (3.29) if $\langle \sigma^i_{rr} \rangle \geq 0$ or in (3.31) if $\langle \sigma^i_{rr} \rangle < 0$.

Given (1.45), according to (3.26), the macrostress $\langle \sigma_{33} \rangle$, macrostrain $\langle \varepsilon_{33} \rangle$, and temperature θ are related by

$$\langle \sigma_{33} \rangle = \frac{1}{\lambda^*_{11} + \lambda^*_{12}} \{[(\lambda^*_{11} + \lambda^*_{12})\lambda^*_{33} - 2(\lambda^*_{13})^2] \langle \varepsilon_{33} \rangle - [(\lambda^*_{11} + \lambda^*_{12})\beta^*_3 - 2\lambda^*_{13}\beta^*_1]\theta\} \tag{3.34}$$

and

$$\langle\varepsilon_{11}\rangle=\langle\varepsilon_{22}\rangle=-\frac{\lambda_{13}^*\langle\varepsilon_{33}\rangle-\beta_1^*\theta}{\lambda_{11}^*+\lambda_{12}^*} \tag{3.35}$$

in (3.30) if $\langle\sigma_{rr}^i\rangle\geq 0$ or (3.32) if $\langle\sigma_{rr}^i\rangle<0$.

Comparing the numerical results with those disregarding the thermal effect [47, 54, 58] shows that the temperature has a significant impact on the stress–strain curves. The temperature θ also strongly affects the behavior of porosity under increasing strain. Thermal loading may cause microdamages even in the absence of mechanical strains.

In the case of deformation and damage induced by thermal loading alone (3.22), the macrostrains $\langle\varepsilon_{11}\rangle,\langle\varepsilon_{22}\rangle,\langle\varepsilon_{33}\rangle$ and the temperature θ are linearly related by

$$\langle\varepsilon_{11}\rangle=\langle\varepsilon_{22}\rangle=\alpha_1^*\theta,\qquad \langle\varepsilon_{33}\rangle=\alpha_3^*\theta. \tag{3.36}$$

Using relations (1.17), (3.10), (3.29), (3.30), and (3.36), we obtain a porosity balance equation for the case of thermal loading, where the stresses $\langle\sigma_{jk}^i\rangle$ are defined by (3.30) and (3.36).

A numerical analysis reveals that thermal loading can cause microdamage even in the absence of macrostresses because the coefficients of linear thermal expansion in the components are different and, thereby, one component is under compression and the other under tension. As a result, microdamages occur in the latter component.

3.4. Fibrous Composite. Let us consider a unidirectional fibrous composite with dispersed microdamages in an isotropic matrix that are modeled by empty pores with porosity p_2. The fibers are transversely isotropic and normal to the isotropy plane x_1x_2. Denote the elastic moduli and the thermal stress and strain coefficients of fibers by $\lambda_{11}^1,\lambda_{12}^1,\lambda_{13}^1,\lambda_{33}^1,\lambda_{44}^1$, β_1^1,β_3^1, α_1^1,α_3^1 and the bulk and shear moduli and the thermal stress and strain coefficients of the undamaged portion of the matrix by $K_2,\mu_2,\beta_2,\alpha_2$, and the volume fractions of fibers and porous matrix by c_1 and c_2, respectively. The macrostrains $\langle\varepsilon_{jk}\rangle$, macrostresses $\langle\sigma_{jk}\rangle$, and temperature θ are related by (3.26). The effective elasticity moduli $\lambda_{11}^*,\lambda_{12}^*,\lambda_{13}^*,\lambda_{33}^*$, and λ_{44}^* of the fibers are defined by (1.48)–(1.50), and the coefficients β_1^*,β_3^* and α_1^*,α_3^* by the following formulas [10, 34, 35, 37]:

$$\beta_1^*=c_1\beta_1^1+c_2\beta_{2p}-\frac{c_1c_2(\lambda_{11}^1+\lambda_{12}^1-2\lambda_{2p}-2\mu_{2p})(\beta_1^1-\beta_{2p})}{2c_1(\lambda_{2p}+\mu_{2p})+c_2(\lambda_{11}^1+\lambda_{12}^1)+2m},$$

$$\beta_3^*=c_1\beta_3^1+c_2\beta_{2p}-\frac{2c_1c_2(\lambda_{13}^1-\lambda_{2p})(\beta_1^1-\beta_{2p})}{2c_1(\lambda_{2p}+\mu_{2p})+c_2(\lambda_{11}^1+\lambda_{12}^1)+2m},$$

$$\alpha_1^*=\frac{\lambda_{33}^*\beta_1^*-\lambda_{13}^*\beta_3^*}{(\lambda_{11}^*+\lambda_{12}^*)\lambda_{33}^*-2(\lambda_{13}^*)^2},\qquad \alpha_3^*=\frac{(\lambda_{11}^*+\lambda_{12}^*)\beta_3^*-2\lambda_{13}^*\beta_1^*}{(\lambda_{11}^*+\lambda_{12}^*)\lambda_{33}^*-2(\lambda_{13}^*)^2}. \tag{3.37}$$

The effective moduli and thermal coefficients of the porous matrix, $K_{2p},\mu_{2p},\beta_{2p},\alpha_{2p}$, are defined by (1.17) and (3.10) ($i=2$).

Assuming that a single microdamage occurs in the undamaged portion of the matrix in accordance with the Schleicher–Nadai failure criterion (2.8) ($i=2$) and using the same line of reasoning as in the cases of homogeneous, particulate, and laminated composites, we can write the porosity balance equation in the form (2.9) ($i=2$), where $\langle\sigma_{jk}^2\rangle$, $\langle\varepsilon_{jk}^2\rangle$, and θ are related by

$$\langle\sigma_{jk}^2\rangle=\lambda_{2p}\langle\varepsilon_{rr}^2\rangle\delta_{ij}+2\mu_{2p}\langle\varepsilon_{ij}^2\rangle-\beta_{2p}\theta\delta_{ij}, \tag{3.38}$$

and $\langle\varepsilon_{jk}^2\rangle$ are related to $\langle\varepsilon_{jk}\rangle$ and θ by the following formulas [10, 34, 35, 37]:

$$\langle\varepsilon_{jk}^2\rangle=\frac{\lambda_{11}^*-\lambda_{12}^*-\lambda_{11}^1+\lambda_{12}^1}{c_2(2\mu_{2p}-\lambda_{11}^1+\lambda_{12}^1)}\langle\varepsilon_{jk}\rangle-\frac{1}{\Delta_2}\{[(\lambda_{11}^*-\lambda_{11}^1)a_1-(\lambda_{12}^*-\lambda_{12}^1)a_2-(\lambda_{13}^*-\lambda_{13}^1)a_3]\langle\varepsilon_{rr}\rangle$$

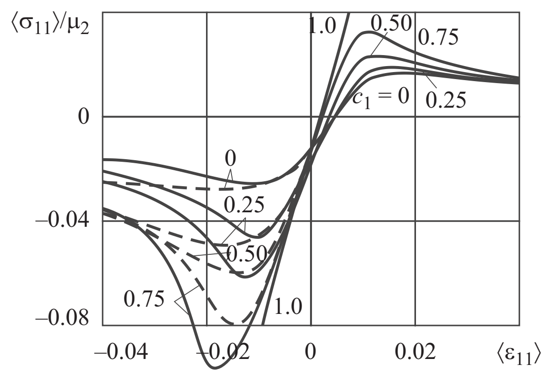

Fig. 24

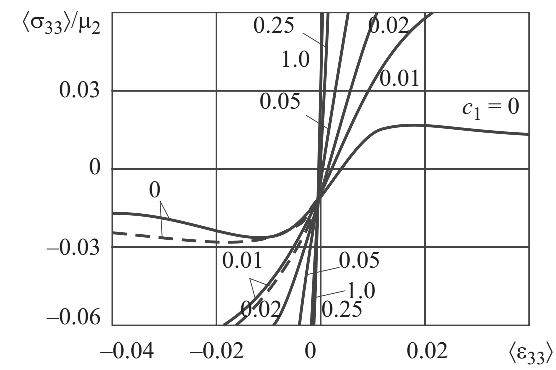

Fig. 25

$$+[(\lambda_{13}^{*}-\lambda_{13}^{1})(a_1-a_2)-(\lambda_{33}^{*}-\lambda_{33}^{1})a_3]\langle\varepsilon_{33}\rangle$$

$$-[(\beta_1^{*}-c_1\beta_1^{1}-c_2\beta_{2p})(a_1-a_2)-(\beta_3^{*}-c_1\beta_3^{1}-c_2\beta_{2p})a_3]\theta\}\delta_{jk},$$

$$\langle\varepsilon_{33}^{2}\rangle=-\frac{1}{\Delta_2}\{[(\lambda_{13}^{*}-\lambda_{13}^{1})a_4-(\lambda_{11}^{*}+\lambda_{12}^{*}-\lambda_{11}^{1}-\lambda_{12}^{1})a_3]\langle\varepsilon_{rr}\rangle$$

$$+[(\lambda_{33}^{*}-\lambda_{33}^{1})a_4-2(\lambda_{13}^{*}-\lambda_{13}^{1})a_3]\langle\varepsilon_{33}\rangle-[(\beta_3^{*}-c_1\beta_3^{1}-c_2\beta_{2p})a_4-2(\beta_1^{*}-c_1\beta_1^{1}-c_2\beta_{2p})a_3]\theta\},$$

$$\langle\varepsilon_{j3}^{2}\rangle=\frac{\lambda_{44}^{*}-\lambda_{44}^{1}}{c_2(\mu_{2p}-\lambda_{44}^{1})}\langle\varepsilon_{j3}\rangle\qquad(j,k,r=1,2),\tag{3.39}$$

where Δ_2, a_1, a_2, a_3, and a_4 are defined by (1.52) and $K_{2p}, \mu_{2p}, \beta_{2p}$, and, α_{2p} by (1.17) and (3.10) ($i = 2$).

We generalize the above model of damaged fibrous composite by assuming that microdamages are pores filled with particles of a damaged material that resist deformation. Then, according to Sec. 1, when $\bar{\sigma}_{rr}^{2p} \geq 0$ (the average bulk stresses in the pores of the matrix are tensile), the effective moduli and thermal coefficients of the porous filled matrix, $K_{2p}, \lambda_{2p}, \mu_{2p}, \beta_{2p}$, are defined by (1.17) and (3.10) ($i = 2$). When $\bar{\sigma}_{rr}^{2p} < 0$ (the stresses are compressive), according to Sec. 2, the effective moduli and thermal coefficients have the form (2.7) and (3.13) ($i = 2$).

Assuming that a single microdamage occurs in the undamaged portion of the matrix in accordance with the Schleicher–Nadai failure criterion (2.8), we arrive at the porosity balance equation (2.9) ($i = 2$), where I_{σ}^{2} is given by (1.38) and $\bar{\sigma}_{rr}^{2}$ by (2.10).

Given the macrostrains $\langle\varepsilon_{jk}\rangle$ and temperature θ, we can use relations (1.53), (3.38), and (3.39) to ascertain whether $\bar{\sigma}_{rr}^{2p} \geq 0$ or $\bar{\sigma}_{rr}^{2p} < 0$. In view of (1.39) and (2.10), the porosity balance equation (2.9) reduces to the form (3.29) when $\bar{\sigma}_{rr}^{2p} \geq 0$, where $K_{2p}, \lambda_{2p}, \mu_{2p}$, and β_{2p} are defined by (1.17) and (3.10), and to the form (3.31) when $\bar{\sigma}_{rr}^{2p} < 0$, where $K_{2p}, \lambda_{2p}, \mu_{2p}$, and β_{2p} are defined by (2.7) and (3.13).

The iterative algorithm (1.25)–(1.29) based on the secant method [4] and on (1.48)–(1.50), (3.37), (1.17), (3.10), (1.19) (or (1.20)), (3.38), (3.39), (1.53), (3.29), and $\langle\sigma_{rr}^{i}\rangle \geq 0$ or (1.48)–(1.50), (3.37), (2.7), (3.13), (1.19) (or (1.20)), (3.38), (3.39), (1.53), (3.31), and $\langle\sigma_{rr}^{i}\rangle < 0$, which are systems of nonlinear algebraic equations for p_2, was used to determine the volume fraction of microdamages in the matrix and the elastic characteristics of the composite and to plot stress–strain curves for a fibrous composite for the Weibull distribution (1.20), different types of loading, and the cases of empty and filled pores. The reinforcement is high-modulus carbon fibers with the elastic characteristics (1.54), volume fractions c_1 = 0, 0.25, 0.5, 0.75, 1.0, and the following transverse and longitudinal thermal strain coefficients [20]:

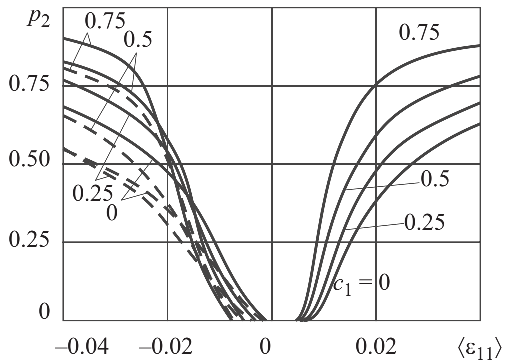

Fig. 26

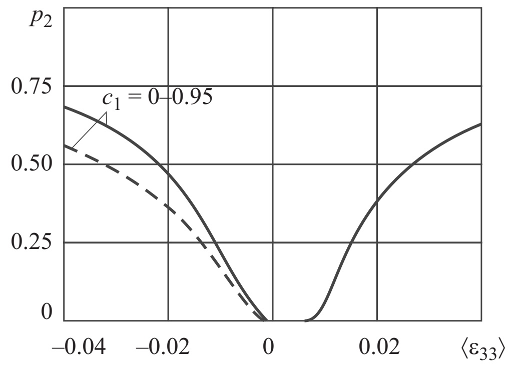

Fig. 27

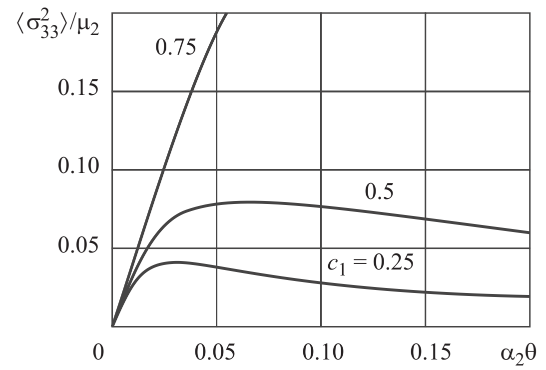

Fig. 28

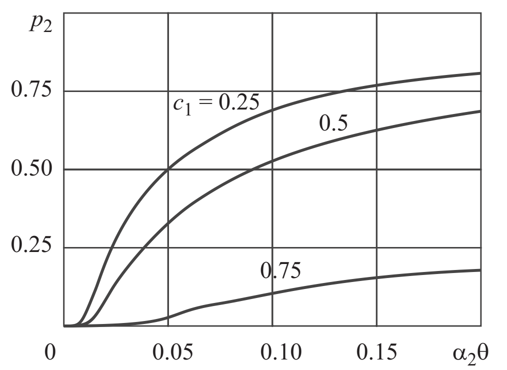

Fig. 29

$$\alpha_1^1 = 18 \cdot 10^{-6}\ {}^\circ\mathrm{C}^{-1}, \qquad \alpha_3^1 = -10 \cdot 10^{-6}\ {}^\circ\mathrm{C}^{-1}, \tag{3.40}$$

which are related to $\lambda_{11}^1, \lambda_{12}^1, \lambda_{13}^1, \lambda_{33}^1, \lambda_{44}^1, \beta_1^1$, and β_3^1 by formulas (1.54) and

$$\beta_1^1 = (\lambda_{11}^1 + \lambda_{12}^1)\alpha_1^1 + \lambda_{13}^1 \alpha_3^1, \quad \beta_3^1 = 2\lambda_{13}^1 \alpha_1^1 + \lambda_{33}^1 \alpha_3^1. \tag{3.41}$$

The material of the matrix is epoxy resin with the characteristics of (1.34), (3.21), (1.35), and $\alpha_2 \theta = 0.0045$.

If condition (1.42) is given, then, according to (3.26), the macrostress $\langle \sigma_{11} \rangle$, macrostrain $\langle \varepsilon_{11} \rangle$, and temperature θ are related by (3.32). In this case, equality (3.33) holds for the porosity balance equation (3.29) if $\langle \sigma_{rr}^i \rangle \geq 0$ and for (3.31) if $\langle \sigma_{rr}^i \rangle < 0$. If condition (1.45) is given, then, according to (3.26), the macrostress $\langle \sigma_{33} \rangle$, macrostrain $\langle \varepsilon_{33} \rangle$, and temperature θ are related by (3.34). In this case, equality (3.35) holds for the porosity balance equation (3.29) if $\langle \sigma_{rr}^i \rangle \geq 0$ and for (3.31) if $\langle \sigma_{rr}^i \rangle < 0$.

Figures 24 and 25 show (for (1.41) and (1.44), respectively) $\langle \sigma_{11} \rangle / \mu_2$ as a function of $\langle \varepsilon_{11} \rangle$ and $\langle \sigma_{33} \rangle / \mu_2$ as a function of $\langle \varepsilon_{33} \rangle$ for different values of c_1 in the cases of tension and compression. In the case of compression, the solid lines correspond to pores filled with particles of a damaged material, and the dashed lines to empty pores. Comparing these curves with those plotted regardless of the thermal effect [55, 59, 76] reveals that temperature has a significant impact on the stress–strain curves. Figures 26 and 27 show (for (1.41) and (1.44), respectively) the porosity p_2 as a function of $\langle \varepsilon_{11} \rangle$ and $\langle \varepsilon_{33} \rangle$ for different values of c_1 in the cases of tension and compression. As can be seen, the temperature θ has a significant effect on the behavior of the curves with increasing strains. Thermal loading may cause microdamages even in the absence of mechanical strains.

In the case of thermally induced deformation and microdamage (3.23), the macrostrains $\langle \varepsilon_{11} \rangle$, $\langle \varepsilon_{22} \rangle$, and $\langle \varepsilon_{33} \rangle$ are related to the temperature θ by (3.38). Using relations (1.17), (3.10), (3.29), (3.38), (3.39), and (1.53), we obtain a porosity balance equation, where $\langle \sigma_{jk}^2 \rangle$ are defined by (1.53), (3.38), and (3.39).

Figures 28 and 29 show the stress $\langle \sigma_{33}^2 \rangle / \mu_2$ in the matrix and its porosity p_2 on the thermal strain $\alpha_2 \theta$, i.e., in the case of thermal effect alone (3.22). As is seen, thermal loading can induce microdamage in the absence of mechanical macrostresses because the coefficients of linear thermal expansion in the components are different and, thereby, one component is under compression and the other under tension. As a result, microdamages occur in the latter component.

REFERENCES

1. L. A. Alekseev and A. A. Svetashkov, "On the deformation theory of filled elastomers with microstructural damages," in: *Solid Mechanics* [in Russian], NII Prikl. Mat. Mekh., Tomsk (1990), pp. 10–20.
2. V. N. Aptukov and V. L. Belousov, "A model of anisotropic damage for bodies. Communication 1. General relationships," *Strength of Materials*, **26**, No. 2, 110–115 (1994).
3. N. N. Afanas'ev, *Fatigue Strength of Metals: Statistical Theory* [in Russian], Izd. AN USSR, Kyiv (1953).
4. Ya. S. Berezikovich, *Approximate Calculations* [in Russian], GITTL, Leningrad–Moscow (1949).
5. A. A. Vakulenko and L. M. Kachanov, "Continuum theory of cracked medium," *Izv. AN SSSR*, *Mekh. Tverd. Tela*, No. 4, 159–166 (1971).
6. S. D. Volkov, *Statistical Theory of Strength* [in Russian], Gos. Izd. Mashinostr. Lit., Sverdlovsk–Moscow (1960).
7. V. P. Golub, "Nonlinear mechanics of damage and its applications," in: *Crack Resistance of Materials and Structural Members* [in Russian], Kyiv (1980), pp. 19–20.
8. V. P. Golub, "Nonlinear models of creep damage accumulation," *Probl. Mashinostr. Avtom*., No. 1, 51–58 (1992).
9. V. P. Golub, "Constitutive equations in nonlinear damage mechanics," *Int. Appl. Mech*., **29**, No. 10, 794–804 (1993).
10. A. N. Guz, L. P. Khoroshun, G. A. Vanin, et al., *Materials Mechanics*, Vol. 1 of the three-volume series *Mechanics of Composite Materials and Structural Members* [in Russian], Naukova Dumka, Kyiv (1982).
11. A. N. Guz, L. P. Khoroshun, M. I. Mikhailova, D. V. Babich, and E. N. Shikula, *Applied Research*, Vol. 12 of the 12-volume series *Mechanics of Composite Materials* [in Russian], A.S.K., Kyiv (2003).
12. N. N. Davidenkov, *Fatigue of Metals* [in Russian], Izd. AN USSR, Kyiv (1947).
13. L. M. Kachanov, *Fundamentals of Fracture Mechanics* [in Russian], Nauka, Moscow (1974).
14. J. A. Collins, *Failure of Materials in Mechanical Design: Analysis*, *Prediction*, *Prevention*, 2nd ed., Wiley-Interscience, New York (1993).
15. V. P. Kogaev, "Fatigue resistance in connection with stress concentration and absolute dimensions," in: *Some Issues of Fatigue Strength* [in Russian], Mashgiz, Moscow (1955).
16. V. I. Kondaurov, "Modeling damage accumulation and dynamic failure of solids," in: *Research into Substance Properties in Extreme Conditions* [in Russian], Moscow (1990), pp. 145–152.
17. T. A. Kontorova and O. A. Timoshenko, "Generalization of statistical strength theory to inhomogeneous stress state," *Zh. Tekhn. Fiz*., **19**, No. 3, 5–31 (1949).
18. T. A. Kontorova and Ya. I. Frenkel', "Statistical brittle fracture theory for real crystals," *Zh. Tekhn. Fiz*., **11**, No. 3, 173 (1941).
19. I. M. Kop'yev and A. S. Ovchinskii, *Failure of Fiber-Reinforced Metals* [in Russian], Nauka, Moscow (1977).
20. A. F. Kregers, "Mathematical modeling of the thermal expansion of spatially reinforced composites," *Mech. Comp. Mater*., **24**, No. 3, 316–325 (1988).
21. S. A. Lurie, "On one entropy model of damage accumulation in a composite," in: *Abstracts 3rd All-Union Conf. on Mechanics of Inhomogeneous Structures* (Lvov, September 17–19, 1991), Pt. 2, Lvov (1991), p. 198.
22. S. A. Lurie, I. M. Krivolutskaya, and A. R. Vvedenskii, "On one micromechanical entropy model of dispersed damages accumulated in composite materials," *Tekhnologiya*, *Ser. Konstr. Komp. Mater*., No. 1, 5–12 (1995).
23. E. S. Pereverzev, *Damage Accumulation Models in Endurance Problems* [in Russian], Naukova Dumka, Kyiv (1995).
24. Yu. M. Rabotnov, *Creep of Structural Members* [in Russian], Nauka, Moscow (1966).
25. A. R. Rzhanitsyn, *Theory of Structural Reliability Design* [in Russian], Stroiizdat, Moscow (1978).
26. R. D. Salganik, "Mechanics of bodies with a great number of cracks," *Izv. AN SSSR*, *Mekh. Tverd. Tela*, No. 4, 149–158 (1973).

27. L. G. Sedrakyan, *Statistical Strength Theory Revisited* [in Russian], Izd. Arm. Inst. Stroimater. Sooruzh., Yerevan (1958).
28. S. V. Serensen, *Fatigue of Metals* [in Russian], Izd. VNIITMASH, Moscow (1949).
29. N. K. Snitko, "On structural theory of strength of metals," *Zh. Tekhn. Fiz*., **18**, No. 6, 857 (1948).
30. V. P. Tamuzs, "Calculation of elasticity parameters of a material with defects," *Mech. Comp. Mater*., **13**, No. 5, 702–707 (1977).
31. V. P. Tamuzs and V. S. Kuksenko, *Microfracture Mechanics of Polymer Materials* [in Russian], Zinatne, Riga (1978).
32. Ya. B. Fridman, *Unified Theory of Metal Strength* [in Russian], Oborongiz, Moscow (1952).
33. L. P. Khoroshun, "Saturated porous media," *Int. Appl. Mech*., **12**, No. 12, 1231–1237 (1976).
34. L. P. Khoroshun, "Methods of theory of random functions in problems of macroscopic properties of microinhomogeneous media," *Int. Appl. Mech*., **14**, No. 2, 113–124 (1978).
35. L. P. Khoroshun, "Conditional-moment method in problems of the mechanics of composite materials," *Int. Appl. Mech*., **23**, No. 10, 989–996 (1987).
36. L. P. Khoroshun, "Fundamentals of thermomechanics of porous saturated media," *Int. Appl. Mech*., **24**, No. 4, 315–325 (1988).
37. L. P. Khoroshun, B. P. Maslov, E. N. Shikula, and L. V. Nazarenko, *Statistical Mechanics and Effective Properties of Materials*, Vol. 3 of the 12-volume series *Mechanics of Composite Materials* [in Russian], Naukova Dumka, Kyiv (1993).
38. L. P. Khoroshun and E. N. Shikula, "Deformation of particulate composites with microdamages," in: *Proc. Int. Conf. on Dynamic Systems: Modeling and Stability Investigation*, Kyiv, May 25–29 (1999), p. 79.
39. L. P. Khoroshun and E. N. Shikula, "Influence of temperature on the microdamage of a particulate material," *Visn. Kyiv. Univ*., *Ser. Fiz.-Mat. Nauky*, No. 5, 382–387 (2001).
40. L. P. Khoroshun and E. N. Shikula, "Short-term microdamage of particulate composites under thermal loads," in: *Proc. Int. Conf. on Dynamic Systems: Modeling and Stability Investigation*, Kyiv, May 22–25 (2001), p. 335.
41. L. P. Khoroshun and E. N. Shikula, "Influence of temperature on the short-term microdamage of laminated materials," *Teor. Prikl. Mekh*., No. 37, 50–58 (2003).
42. L. P. Khoroshun and E. N. Shikula, "Coupled processes of deformation and microdamageability of physically nonlinear materials," in: *Proc. Int. Conf. on Dynamic Systems: Modeling and Stability Investigation*, Kyiv, May 27–30 (2003), p. 370.
43. L. P. Khoroshun and E. N. Shikula, "Structural theory of short-term microdamageability of physically nonlinear composites," in: *Proc. Int. Conf. on Dynamic Systems: Modeling and Stability Investigation*, Kyiv May 23–25 (2005), p. 346.
44. B. B. Chechulin, "Statistical brittle fracture theory revisited," *Zh. Tekhn. Fiz*., **24**, No. 2, 31–37 (1954).
45. E. M. Shevadin, I. A. Razov, R. E. Reshetnikova, and B. I. Serpenikov, "On the nature of the scale effect in metal failure," *Dokl. AN SSSR*, **113**, No. 5, 1057 (1957).
46. E. N. Shikula, "Influence of the strength distribution law on the deformation of a particulate composite with microdamages," *Dop. NAN Ukrainy*, No. 4, 88–93 (1998).
47. E. N. Shikula, "Dependence of the elastic properties of a laminated composite on the strength distribution law in the components," *Dop. NAN Ukrainy*, No. 5, 70–74 (1998).
48. S. Basle and B. Audoin, "On internal variables in anisotropic damage," *Eur. J. Mech. A/Solids*, **10**, No. 6, 587–606 (1991).
49. S. Chandrakanth and P. C. Pandey, "An isotropic damage model for ductile material," *Eng. Fract. Mater*., **50**, No. 4, 457–465 (1995).
50. A. N. Guz, "On one two-level model in the mesomechanics of cracked composites," *Int. Appl. Mech*., **39**, No. 3, 274–285 (2003).
51. L. P. Khoroshun, "Principles of the micromechanics of material damage. 1. Short-term damage," *Int. Appl. Mech*., **34**, No. 10, 1035–1041 (1998).
52. L. P. Khoroshun, "Micromechanics of short-term thermal microdamageability," *Int. Appl. Mech*., **37**, No. 9, 1158–1165 (2001).

53. L. P. Khoroshun and E. N. Shikula, “Effect of the strength scatter of the components on the deformation of a particulate composite with microcracks,” *Int. Appl. Mech*., **33**, No. 8, 626–631 (1997).
54. L. P. Khoroshun and E. N. Shikula, “Effect of the spread of the strength of the components on the deformation of a laminar composite with microfailures,” *Int. Appl. Mech*., **33**, No. 9, 679–684 (1997).
55. L. P. Khoroshun and E. N. Shikula, “Effect of the random character of the microscopic strength of the binder on the deformation of a fiber composite,” *Int. Appl. Mech*., **33**, No. 10, 788–793 (1997).
56. L. P. Khoroshun and E. N. Shikula, “Effect of the spread of strength characteristics of the binder on the deformation of laminar-fibrous materials,” *Int. Appl. Mech*., **34**, No. 1, 39–45 (1998).
57. L. P. Khoroshun and E. N. Shikula, “The theory of short-term microdamageability of granular composite materials,” *Int. Appl. Mech*., **36**, No. 8, 1060–1066 (2000).
58. L. P. Khoroshun and E. N. Shikula, “Simulation of the short-term microdamageability of laminated composites,” *Int. Appl. Mech*., **36**, No. 9, 1181–1186 (2000).
59. L. P. Khoroshun and E. N. Shikula, “Short-term microdamageability of fibrous composites with transversally isotropic fibers and a microdamaged binder,” *Int. Appl. Mech*., **36**, No. 12, 1605–1611 (2000).
60. L. P. Khoroshun and E. N. Shikula, “The micromechanics of short-term damageability of fibrolaminar composites,” *Int. Appl. Mech*., **36**, No. 5, 638–646 (2001).
61. L. P. Khoroshun and E. N. Shikula, “A note on the theory of short-term microdamageability of granular composites under thermal actions,” *Int. Appl. Mech*., **38**, No. 1, 60–67 (2002).
62. L. P. Khoroshun and E. N. Shikula, “Short-term microdamageability of laminated materials under thermal actions,” *Int. Appl. Mech*., **38**, No. 4, 432–439 (2002).
63. L. P. Khoroshun and E. N. Shikula, “Short-term microdamageability of fibrous materials with transversely isotropic fibers under thermal actions,” *Int. Appl. Mech*., **38**, No. 6, 701–709 (2002).
64. L. P. Khoroshun and E. N. Shikula, “Short-term damage micromechanics of laminated fibrous composites under thermal actions,” *Int. Appl. Mech*., **38**, No. 9, 1083–1093 (2002).
65. L. P. Khoroshun and E. N. Shikula, “Theory of short-term microdamage for a homogeneous material under physically nonlinear deformation,” *Int. Appl. Mech*., **40**, No. 4, 388–395 (2004).
66. L. P. Khoroshun and E. N. Shikula, “Short-term microdamageability of granular material under physically nonlinear deformation,” *Int. Appl. Mech*., **40**, No. 6, 656–663 (2004).
67. L. P. Khoroshun and E. N. Shikula, “Influence of physically nonlinear deformation on short-term microdamage of a laminar material,” *Int. Appl. Mech*., **40**, No. 8, 878–885 (2004).
68. L. P. Khoroshun and E. N. Shikula, “Influence of physically nonlinear deformation on short-term microdamage of a fibrous material,” *Int. Appl. Mech*., **40**, No. 10, 1137–1144 (2004).
69. L. P. Khoroshun and E. N. Shikula, “Deformation of particulate composite with physically nonlinear inclusions and microdamageable matrix,” *Int. Appl. Mech*., **41**, No. 2, 111–117 (2005).
70. L. P. Khoroshun and E. N. Shikula, “Influence of the physical nonlinearity of the matrix on the deformation of a particulate composite with microdamageable inclusions,” *Int. Appl. Mech*., **41**, No. 4, 345–351 (2005).
71. L. P. Khoroshun and E. N. Shikula, “Deformation of a laminated composite with a physically nonlinear reinforcement and microdamageable matrix,” *Int. Appl. Mech*., **41**, No. 11, 1246–1253 (2005).
72. L. P. Khoroshun and E. N. Shikula, “Short-term microdamage of laminated material with nonlinear matrix and microdamaged reinforcement,” *Int. Appl. Mech*., **41**, No. 12, 1331–1338 (2005).
73. L. P. Khoroshun and E. N. Shikula, “Deformation of fibrous composite with physically nonlinear fibers and microdamageable matrix,” *Int. Appl. Mech*., **42**, No. 1, 32–39 (2006).
74. L. P. Khoroshun and E. N. Shikula, “Short-term microdamageability of a fibrous composite with physically nonlinear matrix and microdamaged reinforcement,” *Int. Appl. Mech*., **42**, No. 2, 127–135 (2006).
75. E. N. Shikula, “Dependence of the deformational properties of a fiber composite on the binder strength distribution,” *Int. Appl. Mech*., **34**, No. 2, 129–135 (1998).
76. E. N. Shikula, “Dependence of the strain properties of fibrous composite laminates on the fiber-strength distribution law,” *Int. Appl. Mech*., **34**, No. 3, 250–256 (1998).
77. W. A. Weibull, “A statistical theory of the strength of materials,” *Proc. Roy. Swed. Inst. Eng. Res*., No. 151, 5–45 (1939).